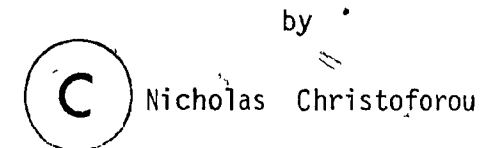
ELECTRICAL CHARACTERIZATION OF GaAs GROWN BY VAPOUR PHASE EPITAXY



A thesis submitted to the Faculty of Graduate Studies and Research in partial fulfilment of the requirements for the degree of Master of Science

Department of Physics *McGill University
Montreal, Quebec, Canada

ς⊬μου

ABSTRACT

Electrical characterization of n-type GaAs single crystals with high impurity concentration was made and the experimental set-up required is described. The electrical behavior of the investigated samples is explained by a two-band conduction, the second being the impurity band where metallic-like conductivity was observed at very low temperatures. The total impurity concentration, as well as the compensation ratio are deduced from the value of the mobility due to ionized-impurity scattering. Also, the ionization energy of the donor impurities is estimated from the temperature dependence of the conductivity at low temperatures.

RESUME

Nous avons mesuré les caractéristiques électriques de monocristaux de GaAs, de type n avec une forte concentration d'impurêtés. Nous donnons une description de l'appareillage nécessaire aux mesures. Le comportement électrique des échantillons mesurés est analysé à l'aide d'un modèle à deux bandes, la seconde étant une bande d'impuretés où on observe, à très basse température, une conductivité de type métallique. La concentration totale en impuretés ainsi que le rapport de concentration sont déduits de la valeur de la mobilité, qui est due à la diffusion par impuretés ionisées. De plus, l'énergie d'ionisation des donneurs est estimée à partir de la dependance en température de la conductivité dans la région des basses températures.

ACKNOWLEDGEMENTS

I am indebted to many people for the assistance I have received in preparing and writing the present thesis. I am, in particular, indebted to my supervisor, Professor D. Walsh, whose advice and guidance greatly enhanced my work. I would also like to extend my gratitude to the Solid State group of the Physics Department of McGill University and especially to J. Auclair, research assistant, F. Van Gils, technician, and M. Baibich, whose technical advice was very helpful. The help of my friends, T. Kefalas and S. Prodromou in making most of the graphs is greatly appreciated. Many thanks also to Joanne Hay for her excellent typing.

The financial support was from the Physics Department of McGill University, as well as from NSERC in the form of a strategic energy grant of a high efficiency GaAs Photovoltaic Cell. I would truly like to thank both of them.

TABLE OF CONTENTS

ABSTRACT.		· i
RESUME		, ii
ACKNOWLEDGEME	NTS	iii
CHAPTER I	Introduction	1
CHAPTER II	Elements of Semiconductor Physics	
	2.1 Energy bands and impurity energy levels	3
	2.2 Carrier concentration— Mott transition	6
	2.3 Electrical transport phenomena	15
	2.4 Measurements of transport properties	24
	2.5 Crystal growth by Organometallic-Vapour	
	Phase Epitaxy (OM—VPE)	27
CHÁPTER III	Experimental apparatus and procedure .	*
	3.1 Crystal growth apparatus	30
	3.2 Contact deposition apparatus	` 32
	3.3 The Cryogenic Temperature Control system .	32
	3.4 The Magnet Control system	. 36
	3.5 The Electrical Measuring Circuit	36
٠ .	3.6 Preparation of the samples	40
	3.7 Hall measurements	41
CHÀPTER IV	Experimental results and discussion	**
	4.1 Temperature dependence of resistivity,	1
	Hall coefficient and Hall mobility	45
	4.2 Calculation of the activation energy ϵ_1	53
	4.3 Calculation of total impurity concentration	r
	and compensation	- 60

CHAPTER V - Conclusion

REFERENCES

65

.).

CHAPTER I

INTRODUCTION

A wide range of contemporary technology, the technology of electronics, is based on materials which are neither metals nor insulators. Such materials are called semiconductors and their electrical properties are intermediate between those of metals and insulators. This is because of the peculiar energy-band structure of the semiconductors as we will see in Chapter II.

One of the semiconductors, with increasing importance in the last decade, is GaAs, some applications of which are Gunn diodes, FET's, LED's and Lasers. Currently, some research is directed towards high-efficiency GaAs solar cells. So, many studies have been made on this material in the last 15 years concerning either the growth technique or its physical properties (1).

The present work is the electrical characterization of n-type GaAs single crystals, grown by Organometallic-Vapor Phase Epitaxy (OM-VPE). This is made by Hall-effect measurements for temperatures ranging from 5 °K to room temperature. The mobility, resistivity, carrier concentration are found, as well as their temperature dependence. From mobility and carrier concentration, the total impurity concentration is estimated. The results are interpreted in terms of the existing theory concerning moderate doped semiconductors, suitably adjusted for our two-band model.

In Chapter II, elements of the physics of semiconductors are reviewed.

In the last part of this chapter, a brief discussion is made about the crystal growth by the Organometallic-Vapor Phase Epitactic (OM-VPE)

technique.

Chapter III is devoted to a description of the growth technique, the experimental apparatus used for the Hall measurements and the experimental process.

In Chapter IV, the various parameters are listed and a discussion, as well as the above-mentioned interpretation of the experimental results are made.

Finally, any tonclusions of the present work are discussed in Chapter V.

ELEMENTS OF SEMICONDUCTOR PHYSICS

2.1. Energy bands and inpurity energy levels.

It is known by X-ray and other studies that most metals and semiconductors are crystalline in structure. A crystal consists of a space array of atoms or ions built up by regular repetition in three dimensions of some fundamental structural unit. It is known also, that for a free isolated atom the electrons are bound to their nucleus only and, hence \mathbf{x} they occupy definite states separated by discrete quanta of energy. Yet, the same is not true for a crystal. This is so, because the potential characterizing the crystalline structure is now a periodic function in space, the value of which at any point is the result of contributions from every atom. When the atoms come close to each other to form the crystal, then, while the energy levels of the inner-shell electrons are not affected appreciably, the levels of the outer-shell electrons are changed considerably, since these electrons now are shared by more than one atom in the crystal. is found by means of quantum mechanics that coupling between the outershell electrons of the atoms results in groups of closely spaced energy states. Each group of them forms a band of continuous levels.

In some materials these bands overlap each other, therefore all values of energy are allowable for the electrons. These materials are metals. If for a pure material, on the other hand, there is a large energy gap ("forbidden band") between the highest occupied electronic state at T=0 and the lowest unoccupied one, then this material is an insulator. The energy gap of an insulator is of order 5-10 eV.

When this energy gap is about 1 or 2 eV, then the material is a semiconductor. In this case, the highest occupied band at T=0 is called valence band, which is completely full, and thus conduction is not possible, while the lower unoccupied band is called conduction band. Conduction is made by activating electrons from the valence to the conduction band.

The most common semiconductors are elements from the group IV of the Periodic Table, mainly Si and Ge, III-V compounds, such as GaAs, InP, InSb etc. and II-VI compounds such as ZnSe, ZnTe, CdS etc.

The above distinction between a semiconductor and an insulator is purely quantitave and, to a large extent, conventional. So, at temperature of 0 $^{\circ}$ K, even this forbidden band of $^{\circ}$ l eV is too large for an electron to "jump" from the valence to the conduction band, and thus this material behaves like an insulator at that temperature.

As we increase the electron energy by a variety of methods (temperature increase, irradiation, illumination), then some electrons "jump" from the valence to the conduction band, leaving behind positive holes. In such case, the resultant conductivity is known as intrinsic conductivity and the material as an intrinsic semiconductor.

The motion of these particles (electrons or holes) inside the crystal, is viewed by quantum mechanics as the motion of a free particle having mass

$$m^* = \frac{\hbar^2}{d^2 E/dk^2}$$

where E is the energy of the particle and The its momentum. This mass m* is called effective mass of the particle.

Also, the conductivity can be altered by introducing certain impurity atoms in the semiconductor; when a foreign atom with one electron more in the outer shell than the atom which it replaces in the host crystal, (e.g. Si replacing Ga in GaAs), is introduced, then this electron is under the influence of the electrostatic force with the positive nucleus of the impurity atom reduced however by the dielectric constant χ of the medium. Moreover its mass is considered to be not its free mass, but the effective mass m*. Using a hydrogenic model the binding energy of the 1s ground state is given by

$$E_{1s} = \frac{m^* e^4}{2h^2 \chi^2} \sim 5.5 \text{ meV} \qquad \text{for GaAs}$$

Here we take $m^* = 0.07m$ and $\chi = 13$ for GaAs. This energy is considerably lower than the energy gap ($E_G = 1.43$ eV for GaAs at 300 °K), and thus the introduction of these impurities results in allowable energy states within the forbidden band and close to the conduction band. These impurities are called donors.

On the other hand, if the impurity atom has one electron less than the replaced one, (e.g. C replacing As in GaAs), then its introduction to the crystal result in allowable states near the valence band, and hence electrons may easily be excited from the valence band to this state leaving behind holes. Generally, this energy is higher than the previous since the hole effective mass is larger than the electron effective mass. The impurities which supply the semiconductor with holes are called acceptors.

The most common dopants for GaAs are elements from the VI group of the Periodic Table (e.g. Se, Te etc.) which act as donors replacing As and those from the II group (Zn, Cd etc) form acceptors when they replace Ga. Impurities from the IV group act either as donors or as acceptors depending on which matrix atom they replace. A complete table of the various impurities and their ionization energy for GaAs is given by Sze⁽²⁾. The different values of the ionization energy for each impurity are due to the deviation of the impurity atom from the hydrogen model we considered before.

2.2. Carrier concentration - Mott transition

As we have already said the conductivity of a semiconductor depends on the total number of electrons (holes), which exist in the conduction (valence) band. This free carrier concentration is governed by some statistical laws.

A key for studying the carrier concentration is the Fermi energy F. We can define it as the energy level with half probability to be occupied and half to be unoccupied. The position of this level depends on the doping and temperature. If we denote $E_{\mathcal{C}}$ the bottom of the conduction band, then the probability to be occupied is according to Fermi-Dirac distribution function

$$f(E_c,T) = \frac{1}{\frac{E_c-F}{kT}} \exp(\frac{1}{kT}) + 1$$
 (2.1)

where k is the Boltzmann constant.

For a slightly doped semiconductor where the Fermi level is considerably lower than E_c , yet considerably higher than the top E_v of the valence band (non-degenerate case), eq. (2.1) reduces to the classical

Maxwell-Boltzmann distribution function:

$$f(E_c,T) \sim \exp(-\frac{E_c-F}{kT}) \tag{2.2}$$

If we restrict ourselves to spherical constant-energy surfaces with E_{\min} at the centre of the Brillouin Zone, we have for the electron concentration

$$n = N_c \exp\left(-\frac{E_c - F}{kT}\right)$$
 (2.3).

where N_{C}^{\bullet} is the effective density of states in the conduction band and it is defined as

$$N_{c} = 2(\frac{2\pi m_{e}^{*}kT}{h^{2}})^{3/2} \qquad (2.4)$$

For hole concentration we have

$$p = N_{V} \exp(-\frac{F - E_{V}}{kT})$$
 (2.5)

where

$$N_V = 2(\frac{2\pi m_h^* kT}{h^2})^{3/2}$$

is the effective density of states in the valence band.

In the above formulas m_e^* and m_h^* are the effective masses for the electron and hole respectively.

We see from eq. (2.3) and (2.5) that the product

$$np = N_c N_v \exp(-\frac{E_G}{kT})$$
 (2.6)

where $E_G = E_C - E_V$ is the energy gap, is independent of the Fermi level and hence of the doping.

For an intrinsic semiconductor,

$$n = p = n_1 = \sqrt{N_c N_v} \exp(-\frac{E_G}{2kT})$$
 (2.7)

and the Fermi level is at the middle of the energy gap at T=0. From eq. (2.6) the concentration of one type of carrier can be found if the concentration of the other type is known.

Let us consider now a semiconductor doped with two types of impurities (partly compensated). Let us assume, also, for the rest of this paragraph that $N_D > N_A > n$ where $N_D > N_A$ are the concentrations of donors and acceptors respectively (n-type semiconductor).

An electron now occupying a donor level has a wave function localized about the impurity state and an energy slightly below the conduction band minimum as we have seen in paragraph 2.1. By the "localized" level we mean that each characteristic solution of the Schrödinger equation for an electron in this field decays exponentially to zero at some distance from a point in space.

If we start from sufficiently high temperature, the intrinsic concentration dominates, i.e. $n_i >> N_D - N_A$ and then $n \sim p$ and this is given by eq. (2.7). As the semiconductor is cooled, $n_i \rightarrow 0$ and at certain temperature there is no case of electron excitation from the valence to the conduction band. Regarding the electrons of the donors, some of them will fill the acceptor states and the remainder $(N_D - N_A)$ will "jump" to the conduction

band, assuming that there is enough energy for this. Thus, the electron concentration will be constant for a certain temperature range (exhaustion range) and this is:

$$n = N_D - N_A \tag{2.8}$$

As the temperature is lowered, some of these electrons will fall back to the donor states and the carrier concentration is given by

$$\frac{n(n + N_A)}{N_D - N_A - n} = \frac{N_C}{2} \exp(-\frac{\Delta E_D}{kT})$$
 (2.9)

where $\Delta E_D^{}$ = $E_c^{}$ - $E_D^{}$ is the ionization energy of the donors.

For very low temperatures, where the carriers "freeze", this is given by

$$n = \frac{N_D - N_A}{N_A} \frac{N_C}{2} \exp(-\frac{\Delta E_D}{kT})$$
 (2.10)

A plot of the Fermi level and electron concentration against temperature for the GaAs is given by $Nag^{(3)}$.

Let us see now what happens as the impurity concentration increases. In this case the impurity donors come closer, so there is a small, but finite, overlap between the wave function of electrons of neighbouring donors. In this case, although at very low temperatures there are no electrons in the conduction band, a conduction process is still possible under certain circumstances in which the electron moves between centres by a tunnel effect without activation into the conduction band. This is called impurity conduction (4).

The above mentioned circumstances is due to the presence of compensation. In this case, since N_A electrons have fallen down to the acceptor states, it is possible for one electron to move from an occupied donor level to an unoccupied one. This process is called impurity conduction by hopping process $^{(4)}$ and the interaction with phonons is essential for this. If there is no compensation, impurity conduction is not possible, unless the overlap between the centres is very large, which means a high enough impurity concentration where the electrons behave like a degenerate electron gas as we will see below.

As the impurity concentration increases, the overlap between the wave functions of the impurity centres become larger and the impurity levels form a band, where the electrons can "jump" and move freely with less energy than the donor ionization energy ΔE_D or even with no energy at all. (fig. l.a). In the latter case, electrons can move freely, even in the limit $T \rightarrow 0$, and a semiconductor can be regarded as a metal because it has a finite conductivity.

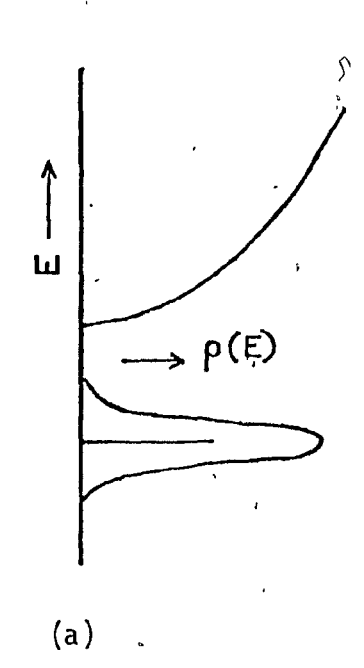
The transition from an insulator to a metal is attributed by Mott to a sharp increase in the number of free electrons to the value n_{cr} , governed by a numerical criterion (5)

$$n_{cr}^{1/3} a_{p} \approx 0.25$$
 (2.11)

where

$$a_0 = h^2 \chi / m^* e^2$$
.

^{*} The term "band" is used somehow incorrectly, since a band is connected with periodic structures. Anyhow, this term will be used with the above reservation.



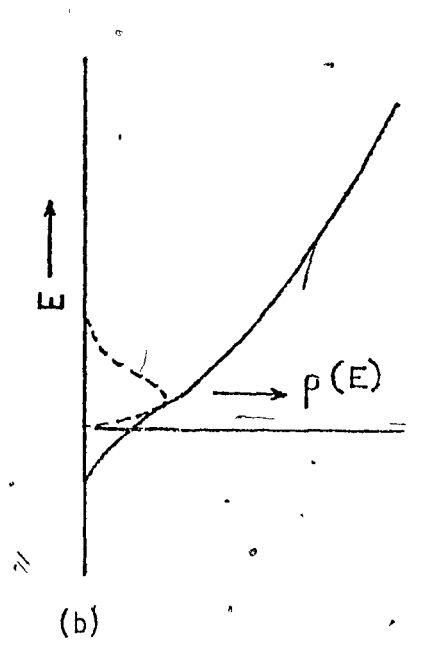


Fig. 1 $^{^{\prime}}$ Formation of the impurity band. $_{\rho}(E)$ is the density of states

Mott derived this criterion assuming the following. If there are no free electrons, then a delocalized electron and the remaining positive hole attract each other with a force behaving at large distances r like $-e^2/\chi r^2$. With a Coulomb force of this kind the electron and the hole always form a bound pair in the lowest energy state and, therefore, they are not able to carry a current at T = 0

On the other hand, if the number of free electrons is sufficiently high, the Coulomb field can be replaced by the screened one

$$-\frac{e^2}{x^r} \exp(-qr)$$

where q is a screening constant and this is so large that there are no bound states. According to Thomas-Fermi model this is given by

$$q^2 = \frac{4m^*e^2n^{1/3}}{\hbar^2x}$$

According to Mott, there are no bound states if $qa_0 \ge 1$. From this limit, (2.11) is derived.

Mott assumed that the metal-non metal transition should be abrupt because a small number of free carriers never exists, since electrons and holes form pairs always with energy of order $m^*e^4/2\hbar^2\chi^2$ (6). The screening mechanism is effective when the concentration reaches the critical value and this occurs suddenly.

The Mott's conclusions differ from the band theory because this theory does not allow for Coulomb interactions between carriers. These interactions are considered by Mott as an attraction between an electron and a localized

hole.

An allowance for the carrier interaction between carriers was first made by $\operatorname{Hubbard}^{(7)}$. He considered the repulsion between electrons located at the same center.

Hubbard considered a Hamiltonian consisting of two parts, $H = H_1 + H_2$. The first part H_1 describes the motion of an electron between neighbouring atoms, without allowance for carrier-carrier Coulomb interaction. The value of H_1 is proportional to the energy-band width \mathcal{E} . The second part H_2 allows for the repulsion between electrons located in the same center and then the energy of the system increases by the repulsion energy U, so H_2 is proportional to U.

If an electron is localized, its kinetic energy increases by an energy of the order of \mathcal{E} . The latter is dependent on the interatomic distance, increasing as the atoms come closer. On the other hand, this localization decreases the potential energy of the electron by the energy U, which is independent of the distance between the atoms.

If U > E, the electron states are localized and the crystal is an insulator. If $U \subseteq E$, the material is a metal. The critical value E/U = 1.15 of this model is close to the Mott criterion, eq. (2.11). The metal-insulator transition, according to Hubbard, can be regarded as the filling of the energy gap between two subbands, one of which is filled and the other empty. The gap between these two subbands decreases as the interatomic distance is reduced.

For even higher impurity concentration, the inpurity band widens greatly. At the same time, the high concentration of ionized donors provides an attractive potential which lowers the edge of the conduction band.

In this case an overlap between this impurity band and the conduction band occurs, becoming greater as the impurity concentration increases (fig. 1.b).

Reviewing eq. (2.11), Fritzsche $^{(8)}$ suggests that instead of using the free carrier concentration, one should consider the total donor concentration N_D; moreover, this critical value of N_D for the metal-insulator transition depends on the compensation, increasing as the latter increases.

In the case of impurity conduction, the conductivity in this model is approximated by a sum of three exponential terms (9)

$$\sigma = C_1 \exp(-\epsilon_1/kT) + C_2 \exp(-\epsilon_2/kT) + C_3 \exp(-\epsilon_3/kT)$$
 (2.12)

where the C_i 's may be temperature-dependent. It is assumed that $\varepsilon_1 > \varepsilon_2 > \varepsilon_3$. The first exponential term represents the conduction-band conductivity, so $\varepsilon_1 = \Delta E_D$. The activation energy ε_2 is the energy required at low temperatures for "intermediate" impurity concentration. A band is formed then by the first excited states $^{(9)}$, separated from other bands, and electron activation into this band gives rise to this term. The mobility is smaller in this band than that of the conduction band but larger than the mobility of the electrons in ground states. The energy ε_2 decreases as the impurity concentration increases and vanishes when the range of ground-state levels merges with the range of the excited states and, hence, the semiconductor has a metallic behaviour.

In addition to the excited states, Fritzsche considers the Upper Hubbard D^- states corresponding to donors, which are negatively charged by binding an extra electron⁽⁹⁾. These D^- states may be lowered due to the

interaction and become important for the conduction in a limited concentration range before they merge with the ground states, the Lower Hubbard D° states, where the metal-insulator occurs.

The activation energy ε_3 is the energy required for the electron motion from one neutral centre to another. As it has already been said, this process can only occur if compensation is present and this is usually a hopping process. Two types of conduction are considered here. In the first, for low compensation, an electron moves from one atom to another of which the energy difference is very small. In the second case, high compensation causes a strongly fluctuating potential in the crystal lattice (10), and the energy difference of neighbouring atoms is considerably larger than that of the former case.

The values of ε_1 , ε_2 and ε_3 decreases as the impurity concentration increases, i.e. when the interatomic distance decreases. As regard the compensation, the values of ε_1 and ε_2 increase with it, while the ε_3 passes through a minimum and then as the compensation continues to increase, the ε_3 increases also (11).

2.3. Electrical transport phenomena

A. Conductivity - Mobility

We saw in the preceding paragraph that the carrier distribution of a semiconductor in thermodynamic equilibrium is given by the classical Maxwell-Boltzmann distribution function for non-degenerate semiconductors, eq. (2.2), or, more generally, by the Fermi-Dirac distribution function, eq. (2.1).

The distribution function is altered when external forces act on the

carriers. In principle, the electronic properties of a conductor are completely specified once this function $f(\vec{k}, \vec{r}, t)$ is known. For example, the current density is given by (12)

$$\vec{J}(\vec{r}, t) = \frac{e}{4\pi^3} \int v_k f(\vec{k}, \vec{r}, t) d\vec{k}$$
 (2.13)

According to Liouville's theorem, electrons which at time t are in $d\vec{r}d\vec{k}$ centered about \vec{r} , \vec{k} , will at time t + dt be located in an equal volume centered about \vec{r} + rdt, \vec{k} + kdt. This difference is due to scattering. Hence, the Botzmann equation (12)

$$\frac{df}{dt} = -\vec{k} \cdot \vec{\nabla}_{k} f - \vec{v} \cdot \vec{\nabla}_{r} f + \frac{\partial f}{\partial t} + (\frac{\partial f}{\partial t})_{c}$$

where the last term indicates the rate of change due to the collision process.

For steady state condition, and under the influence of time-independent forces, then $\partial f/\partial t = 0$, and this equation becomes

$$\stackrel{\rightarrow}{k} \stackrel{\rightarrow}{\nabla}_{k} f + \stackrel{\rightarrow}{v} \stackrel{\rightarrow}{\nabla}_{r} f = \left(\frac{\partial f}{\partial t}\right)_{c}$$
(2.14)

The application of a weak electric field E causes a current density, which is given by inserting the solution of eq. (2.14) into eq. (2.13) and in the relaxation-time approximation

$$\vec{J} = \frac{ne^2}{m^*} \langle \tau \rangle \stackrel{\rightarrow}{E}$$
 (2.15)

where τ is a measure of the rate at which the distribution function relaxes to its normal form. This is called the relaxation time constant for the distribution function and it is defined as (12)

$$\left(\frac{\partial f}{\partial t}\right)_0 = -\frac{f - f_0}{r}$$
 .

From the eq. (2.15), the conductivity is obtained:

$$\sigma = \frac{ne^2}{m^*} < \tau > \tag{2.16}$$

or

$$\sigma = n|e|\mu$$

where, by definition

$$\mu = \frac{|\mathbf{e}| < \tau >}{\mathsf{m}^*} \tag{2.17}$$

 μ is known as mobility. Its usual unit is cm²V⁻¹sec⁻¹.

For two types of carriers the 2nd relation of (2.16) takes the form

$$\sigma = \mathbf{n}|\mathbf{e}|\mu_{\mathbf{e}} + \mathbf{p}|\mathbf{e}|\mu_{\mathbf{h}}$$
 (2.18)

Because the carrier concentration in a semiconductor is generally a sensitive function of temperature and purity, it is preferable to work with the mobility \(\mu \), instead of the conductivity. Then \(\sigmu \) will be given by the second of eq. (2.16) or (2.18).

As relation (2.17) shows, the mobility depends on the relaxation time. The latter is a fundamental parameter in transport phenomena and is a

function only of the energy E of the carriers. Expressions for τ have been derived for various scattering mechanisms. In the following we discuss the major scattering mechanisms.

B. Scattering mechanisms

In an ideal crystal the application of an external field would uniformly accelerate the electron, causing a linear increase of its drift velocity with time in the direction of the field. But it is known that such a linear increase in drift velocity with time does not occur in real crystals. The average electron drift velocity reaches a limiting value, which at low fields is proportional to the magnitude of the field, eq. (2.15). This limit is due to interaction of the electron with crystal imperfections through scattering processes.

These imperfections may be lattice vibrations, defects (crystal defects, impurities, etc) and carrier-carrier interactions. In the first case, where the lattice vibrations are considered, the electrons may collide with acoustical and optical phonons, hence we have the acoustic and optic scattering mechanisms.

These are subdivided further in accordance with the nature of perturbing potentials produced by the vibrations. Acoustic phonons produce the perturbing potential in two ways. First, due to the changing in the spacing of the lattice atoms, the energy band gap, as well as the position of the valence and conduction band edges vary from point to point and due to these potential discontinuities, a potential is produced, which is called deformation potential. Its magnitude is evidently proportional to the produced strain.

The second kind of perturbation is produced by acoustic vibration through piezoelectric effect. In crystal having no inversion symmetry, the displacements of the atoms due to the acoustic vibrations produce an electric field. This effect is important in all compound semiconductors. It is, however, more important in the wurtzite materials (CdS, ZnO) than in the sphalerite ones (InSb, GaAs) because of the lower symmetry of the former.

The optic vibration also produce perturbing potential in two ways.

The first kind, the nonpolar optic scattering is insignificant in most semiconductors. The second kind is more important. Due to its significance in GaAs it will be discussed later.

The second case includes imperfections in the periodic potential in a crystal, which are produced, mainly, during the crystal growth. In properly grown crystals, the effects of the dislocations are negligible compared to those of other imperfections. Here, we shall exclude the collisions at dislocations, but the effect of the impurities will be considered.

As mentioned earlier (paragraph 2.1), the impurity atoms provide energy levels in the forbidden gap, which are occupied by electrons (for donor atoms) and by holes, i.e. are empty, (for acceptor atoms) at very low temperatures. Thus, the collision process is dominated at these temperatures by collisions with the neutral impurity atoms. As the temperature increases, these impurity atoms become ionized, and the collision process is then dominated by the collision of electrons with these ionized atoms. Below, we discuss the effect on mobility due to the polar optical scattering and to the ionized impurities.

i) Folar optical scattering

This scattering occurs mainly in compound semiconductors.

In this case, polarization is produced by the optic vibration due to the ionic charges associated with the atoms forming the compound. The displacement of the neighbouring atoms with the opposite ionic charges results in dipole moments and the associated potential scatters the electrons.

Due to the fact that this scattering mechanism is inelastic, a relaxation time, strictly speaking, cannot be defined, so the temperature dependence of mobility is found by variational techniques.

Petritz and Scanlon using perturbation theory (13) found for polar optical scattering

$$\mu_{p_0} = \frac{8h^2}{3me} \frac{1}{(2\pi mk_0)^{1/2}} \left(\frac{\chi\chi_0}{\chi-\chi_0}\right) \left(\frac{m}{m^*}\right)^{3/2} \frac{\chi(z)(e^z-1)}{z^{1/2}}$$
(2.19)

where Θ is the Debye temperature, χ and χ_0 are the static and optical dielectric constants respectively, $z = \Theta/T$ and

$$x(z) = 1$$
 for $z << 1$
 $x(z) = \frac{3}{8}(\pi z)^{1/2}$ for $z >> 1$

The polar optical scattering is an important scattering mechanism for GaAs in temperature higher than \sim 100 $^{\rm o}{\rm K}.$

ii) Scattering by ionized impurity atoms.

A quantum-mechanical treatment of electronic scattering by ionized impurity atoms has been developed by $Brooks^{(14)}$ and a revision in this approach has been made by Falicov and Cuevas⁽¹⁵⁾.

In his approach, Brooks assumes the scattering process to be perfectly elastic. He assumed that free carriers could collect around a charged centre and screen partly the potential. The theory, originally, was developed for only one kind of impurity (donors) and extended to include both majority (donors) and minority (acceptors) impurities.

Brooks found that, in non-degenerate case, the screening radius should be

$$r_0^2 = \frac{\chi kT}{4\pi e^2 n}$$
 (2.20)

where $\boldsymbol{\chi}$ is the dielectric constant of the crystal and

$$n' = n + (n' + N_A)(1 - \frac{n + N_A}{N_D^a})$$

 N_A denotes acceptor concentration and N_D donor concentration. n is the free electron concentration. If the ionized impurities are randomly arranged in the lattice, they scatter independently, and the total scattering is proportional to the number of impurities. In this case, he found for a spherical energy surface

$$\frac{1}{\tau} = \frac{\pi e^4 N_I}{2^{1/2} V_m * 1/2 E^{3/2}} \left[en(1+b) - \frac{b}{1+b} \right]$$
 (2.21)

where N_{τ} is the total ionized impurity concentration and

$$b = \frac{2m^* \chi kT}{\pi e^2 h^2 n} E \qquad (2.22)$$

The mobility is obtained by substituting eq. (2.21) into eq. (2.17). Since the term in the brackets varies slowly with the carrier energy, a fairly reliable analytic expression for $\mu_{\rm I}$ is obtained, taking E in (2.22) equal to 3kT. Then, according to Brooks

$$\mu_{I(B-H)} = \frac{2^{7/2} \pi^{-3/2} \chi^{2} e^{-3} m^{*-1/2} (kT)^{3/2}}{N_{I} [(2n(1+b)-b(1+b)^{-1}]}$$
(2.23)

To linearize the Poisson's equation Brooks made an approximation which is valid if the electric potential resulting from the ionized impurities is small compared with the thermal energy (14,15). This condition is satisfied in two cases:— at high enough temperatures for any kind of impurity content;— at all temperatures for semiconductors doped with only one kind of impurities.

Falicov and Cuevas proposed a modification of the Brooks-Herring formula, eq. (2.23), in the case for low temperatures and highly compensated materials (15). They assumed pair-correlation function between the acceptors and the donors and they obtained a temperature-independent screening radius

$$r_0' = \frac{1}{2\pi^{1/3} (N_D - N_A)^{1/3}}$$
 (2.24)

Finally, they found for the mobility

$$\mu_{I(F-C)} = \frac{2^{7/2} \pi^{-3/2} \chi^{2} e^{-3} m^{*-1/2} (kT)^{3/2}}{2N_{A} [2n(1+\eta)+\eta(1+\eta)^{-1}]}$$
(2.25)

where.

$$\eta = \frac{6(kT)m^*}{\pi^{2/3}\hbar^2(N_D^{-N}A)^{2/3}}$$
 (2.26)

The eq. (2.25) differs from the Brooks-Herring formula, eq. (2.23) in their denominator and in the fact that the inverse screening radius r_0^{-1} of eq. (2.20) which diverges as T approaches zero, is replaced by that of eq. (2.24) which is independent of temperature.

Above, we discussed the equation which gives the mobility when the ionized impurity scattering is dominant. The importance of this kind of scattering process increases as the temperature of the crystal is increased from very low values. However, as the charge impurity atoms cannot scatter high energy electrons, the effect of ionized impurity atoms decrease again as the temperature is increased to higher values.

C. Combination of mobilities

We discussed above briefly the different scattering mechanisms and we saw the temperature dependence of two of them. Actually in the experimental observations there are deviations from the theoretically expected behaviour. This is because in most semiconductors the constant-energy surfaces are not spherical as we assumed, and of the fact that in all temperature regions more than one scattering mechanisms operate simultaneously.

To calculate the mobility in the latter case, we calculate first the

effective relaxation time, by

$$\frac{1}{\tau_{\text{eff}}} = \Sigma \frac{1}{\tau_{\text{i}}} \tag{2.27}$$

Here, it is assumed that each scattering mechanism acts independently of the other. Now, this $\tau_{\rm eff}$ is inserted into eq. (2.17) to calculate the mobility. From eq. (2.27) we notice that the effective relaxation time is determined by the partial relaxation time which is the smallest under the specific circumstances.

The above calculation often demands numerical methods; an approximate method to calculate the effective mobility is given by the Matthiessen's rule

$$\frac{1}{\mu} = \sum_{i} \frac{1}{\mu_{i}} \qquad (2.28)$$

The latter approximation leads to a small error when two scattering mechanisms are operative, but to a larger one for more scattering mechanisms operative simultaneously.

2.4. Measurements of transport properties -

Electrical conductivity and Hall effect measurements provide the most useful information about the electrical transport properties of semiconductors. To take these measurements it is assumed that the crystal is in isothermic condition and that the electrical conduction is isotropic.

A. Electrical resistivity

For small electric fields, when Ohm's law is valid the resistivity of a sample is given by:

$$\rho = \frac{V_{x}}{I} \frac{t \cdot w}{\ell} \tag{2.29}$$

where V_{χ} is the voltage across the sample contacts a distance ℓ apart, I the current passing through the sample, t and w the thickness and the width of the sample respectively.

The electrical conductivity can then be found by

$$\sigma = \frac{1}{\rho} \tag{2.30}$$

Usual unit for the resistivity of a semiconductor is the α cm (ohm. centimeter) and for the conductivity the inverse, i.e. α^{-1} .cm⁻¹.

B. The Hall effect

If a sample carrying a current I is placed in a transverse magnetic field B, an electric field E_{H} is induced in the direction perpendicular to both I and B. This phenomenon, known as the Hall effect, is used to determine whether a semiconductor is n- or p- type and to find the carrier concentration. Also, by simultaneous measurement of the conductivity σ , the mobility μ can be calculated.

 ${\scriptstyle \times}$ A parameter, the Hall coefficient ${\rm R}_{\rm H}$ is defined as

$$R_{H} = \frac{E_{H}}{JB} \qquad (2.31)$$

where J is the current density.

In the following we assume that carriers of one type are present (e.g. electrons) and that a low magnetic field is applied such as $\mu B << 1$. In this case, the Hall coefficient is equal to

$$R_{H} = \frac{1}{ne} \frac{\langle \tau^{2} \rangle}{\langle \tau \rangle^{2}} = \frac{r_{H}}{ne}$$
 (2.32)

where the factor $r_{\rm H}$ is called Hall factor. We see from eq. (2.32) that the Hall coefficient is inversely proportional to carrier concentration and that its sign coincides with the sign of the carriers. The value or $r_{\rm H}$ is a function of the energy dependence of τ , i.e. depends on the scattering mechanism. Thus, its value is (16)

$$r_{\rm H} = \frac{3\pi}{8} = 1.18$$
 for lattice scattering (2.33)
$$r_{\rm H} = \frac{315\pi}{512} = 1.93$$
 for ionized-impurity scattering

For strong degeneracy, as well as for strong magnetic field $r_{\rm H}$ = 1.

Actually, the value of r_H may be anywhere between 1 and 2 depending on the predominance of the various scattering mechanisms, as $\sqrt{\text{ell}}$ as on the shape of the bands.

Taking the product $R_{H} \cdot \sigma$, we obtain from (2.16) and (2.32)

$$R_{H} = \frac{e}{m_{\Phi}^{\star}} = r_{H}^{2} = r_{H}^{\mu} = \mu_{H}$$
 (2.34)

where μ is the electron drift mobility and $\mu_{\mbox{\scriptsize H}}$ is known as the Hall mobility.

The latter is proportional, but not equal, to μ . The ratio of Hall to drift mobility is given by the value of the Hall factor r_H .

In terms of measured quantities, the Hall coefficient and mobility take the forms

$$R_{H} = \frac{V_{H}t_{,}}{IB}$$
 (2.35)

$$\mu_{H} = \frac{V_{H}}{V_{x}} \frac{\varrho}{w} \frac{1}{B}$$
 (2.36)

The usual units of R_H are cm³/Cb and of the Hall mobility are the same as of the drift (i.e. cm²/V·sec).

2.5 Crystal growth by Organometalic-Vapor Phase Epitaxy (OM-VPE)

Due to the increasing use of the III-V and II-VI compounds in many fields of electronics, many studies have been made for the growth of these crystals. Many reports, for example, have been published on liquid phase epitaxy (LPE), molecular beam epitaxy (MBE) and vapor phase epitaxy (VPE).

In the last decade, many efforts have been made to use metalorganics in preparation of the III-V, and II- 1 I compounds. The first successful and advantageous growth by this technique was reported by Manasevit $^{(17)}$.

He used triethylgallium (TEG) or trimethylgallium (TMG) and group V. hydrides in producing GaAs, GaP, $GaAs_{1-x}P_x$ and $GaAs_{1-x}Sb_x$ on semiconductors and insulators such as sapphire (Al_2O_3) , spinel $(mgAl_2O_4)$ and beryllia (BeO).

Since then, many reports have been published on this new technique, developing it to include more applications, such as homoepitaxial growth

of $GaAs^{(18)}$ and the formation of III-V aluminum compounds and of the II-VI compounds.

The chemical formulae, which describe the OM-VPE reactions, are the * following

2Ga
$$(CH_3)_3 + 3 H_2 \rightarrow 2 Ga + G CH_4$$

(1)

2 Ga + 2 AsH₃ \rightarrow 2 GaAs + 3 H₂

Zn $(CH_3)_2 + H_2 \rightarrow Zn + 2 CH_4$

(2)

Zn + H₂Se \rightarrow ZnSe + H₂

Evidently, the group (1) describe the formation of III-V compounds, while these of group (2) describe the formation of II-VI compounds.

The growth rate depends on the growth temperature, on the substrate and on metalorganic concentration. Manasevit and Simpson found that at any one temperature the growth rate of (111) GaAs on $A\&_2O_3$ is essentially linear with TMG concentration when it is decomposed in an atmosphere containing As and at least a 10-fold excess of $A\sh_3$ over TMG in the gas stream entering the reactor (17).

Many researchers have shown that the electrical characteristics of nominally undoped materials depend on the hydride/organometalic flow-rate ratio. So for GaAs, a flow-rate ratio of AsH_3/TMG equal to 3 gives a p-type material, increasing it to 6 gives an n-type (19). Dopants for the

GaAs are dimethylzinc (DMZ) or diethylzinc (DEZ) giving p-type, and for n-type H₂Se. We notice that the dopants for GaAs, are also used to grow ZnSe.

The advantages of OM-VPE can be summarized as follows,

- (1) reproducible epitactic layers can be grown with a single temperature zone in a quartz reactor at a relatively low temperature, (for example 610 °C for GaAs).
 - (2) the process can be scaled up for industry,
- (3) the same reactor and electronic controls can be used to grow. other III-V and II-VI compounds,
- (4) partial pressures and flow rates of all sources can be controlled externally and
- (5) system is evacuate and if necessary substrate can be plasma etched.

EXPERIMENTAL APPARATUS AND PROCEDURE

3.1. Crystal Growth Apparatus

The apparatus used for the GaAs growth by the Organometallic-Vapor Phase Epitactic (OM-VPE) technique is shown schematically in fig. 2. Generally, this is similar to that reported elsewhere (17). It consists principally of a single vertical quartz tube, the reactor, of dimensions 50 mm in diameter and 60 cm in length. This reactor is equipped with a SiC coated graphite pedestal which can be inductively heated. The latter is supported by a thermocouple by which the temperature can be monitored.

The liquid organometallics are contained in stainless steel bottles, which in turn are kept in thermoelectrically cooled baths; by this way their vapor pressure can be controlled. The carrier gas, which is bubbled through the organometallics, consists of Pd-purified H₂. Its flow, as well as the flows of the hydrides and of the dopants are monitored by appropriate mass-flow valves. A mechanical pump attains the desired pressure under which the growth takes place.

Due to the high toxicity of the reactants, special precautions have been taken. Thus, a pressure gauge sensor (capacitance manometer) monitors the pressure and controls fail-safe solenoid valves of each gas for security reasons. Also, a charcoal trap, placed at the exit of the reactor, traps any toxic As. A 500 lb. charcoal drum is also installed outside the building at the exhaust of the mechanical pump.

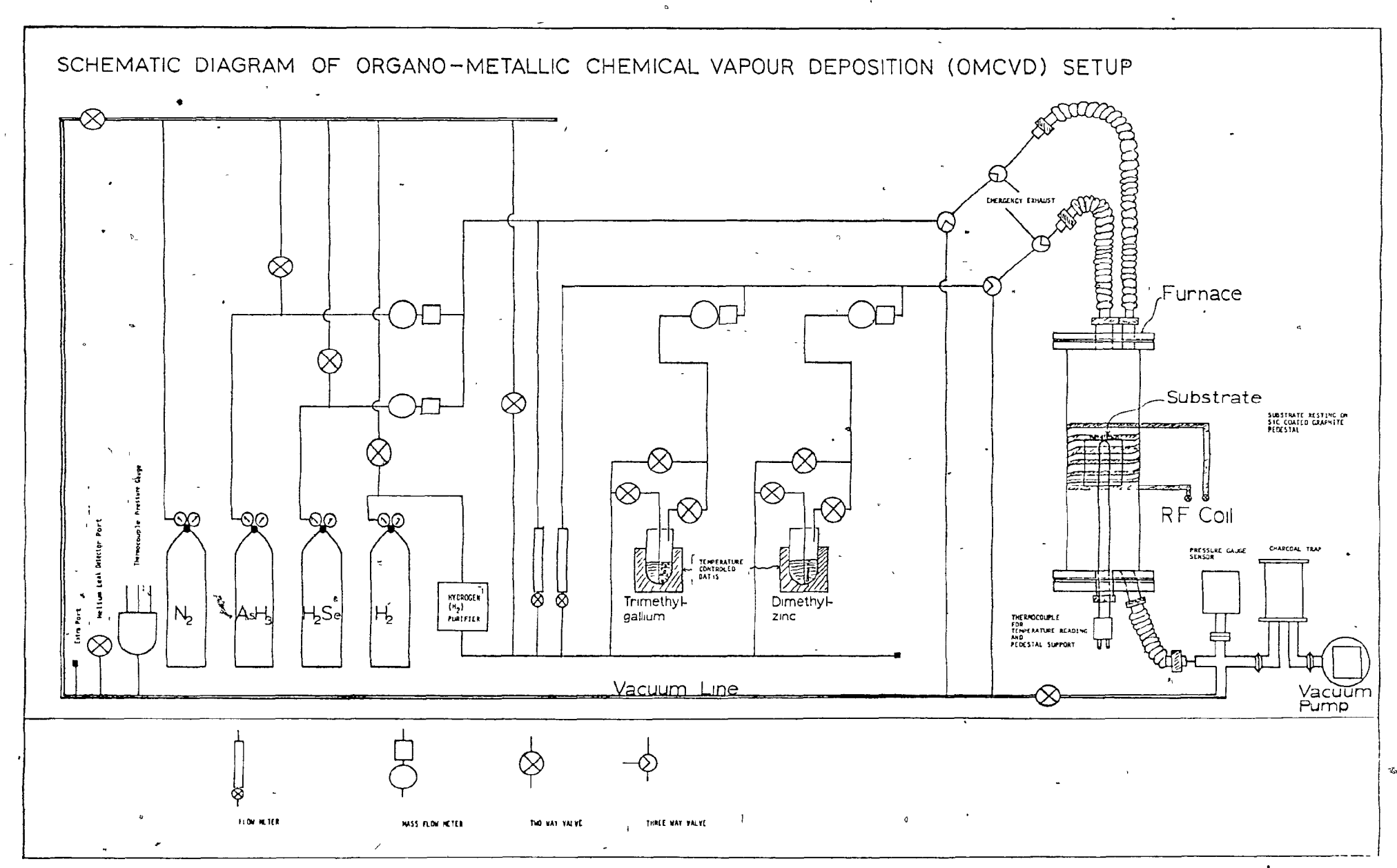


Fig. 2

3.2. Contact Deposition Apparatus

In order to take electrical measurements of a semiconductor, one needs to make ohmic contacts to it. The contacts of the samples investigated were made by vapor deposition or appropriate metals or alloys. The system used for this purpose consists mainly of two components: the electron beam evaporation source and the vacuum system.

The former is a single crucible source using a Varian e-Gun Electron Beam Evaporator. Its power supply has a maximum power of 3 kW with its control unit provided with a convenient single-knob control of evaporation and a water-flow interlock.

The vacuum system is shown schematically in fig. 3. This is composed of the evaporation space and its belljar, the mechanical and diffusion pumps and the cold traps filled with liquid Nitrogen when operating. The pressure is monitored by the gauges, the ion one being used for the range of very low pressure.

3.3. The Cryogenic Temperature Control System

The design of the cryostat used in measuring the electrical resistivity and Hall effect is shown in fig. 4.

The sample is mounted on the end of the support tube F, about 15 mm above the heater G, and lowered into the exchange gas chamber L through an opening at the top of the dewar. All the electrical leads are brought up through insulated tubes located inside the support tube M and are terminated on multipin electrical connectors N. These are hermetically sealed and feature closed-entry socket contacts.

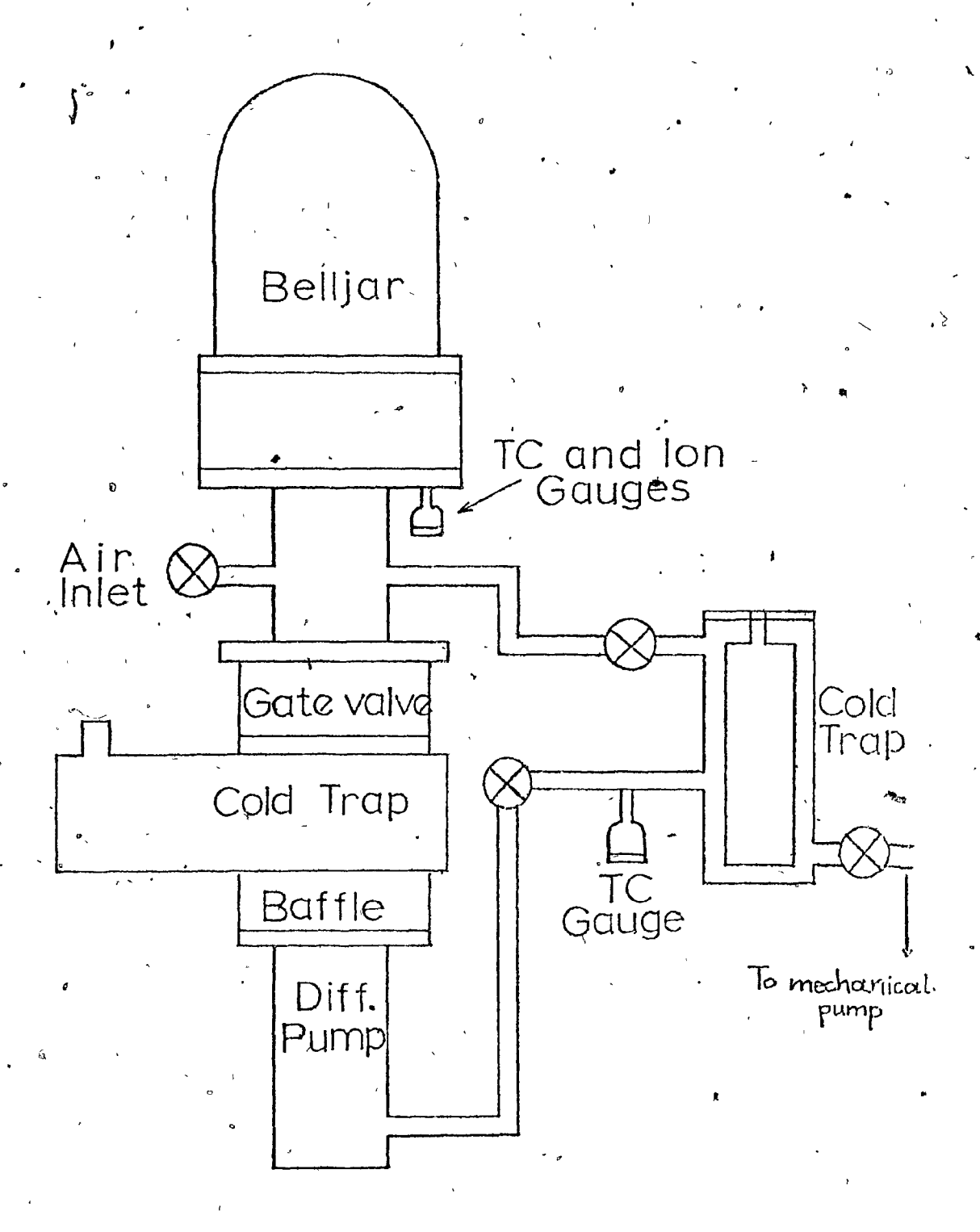


Fig. 3 Vacuum system for contact deposition

Fig. 4

LEGEND

A: Inner wall space of sample chamber

B: Off-gas line

C: Gauges

D; Diffusion pump

'E: Magnet poles

F: Sample place

G: Heater place

H: Liquid Nitrogen reservoir

l: Liquid. Helium reservoir

J: Inner wall space of I

K: Liquid He entry

L: Exchange gas and sample chamber

M: Support tube

N: Electrical connectors

P.: Air inlet

Œ

: Valve

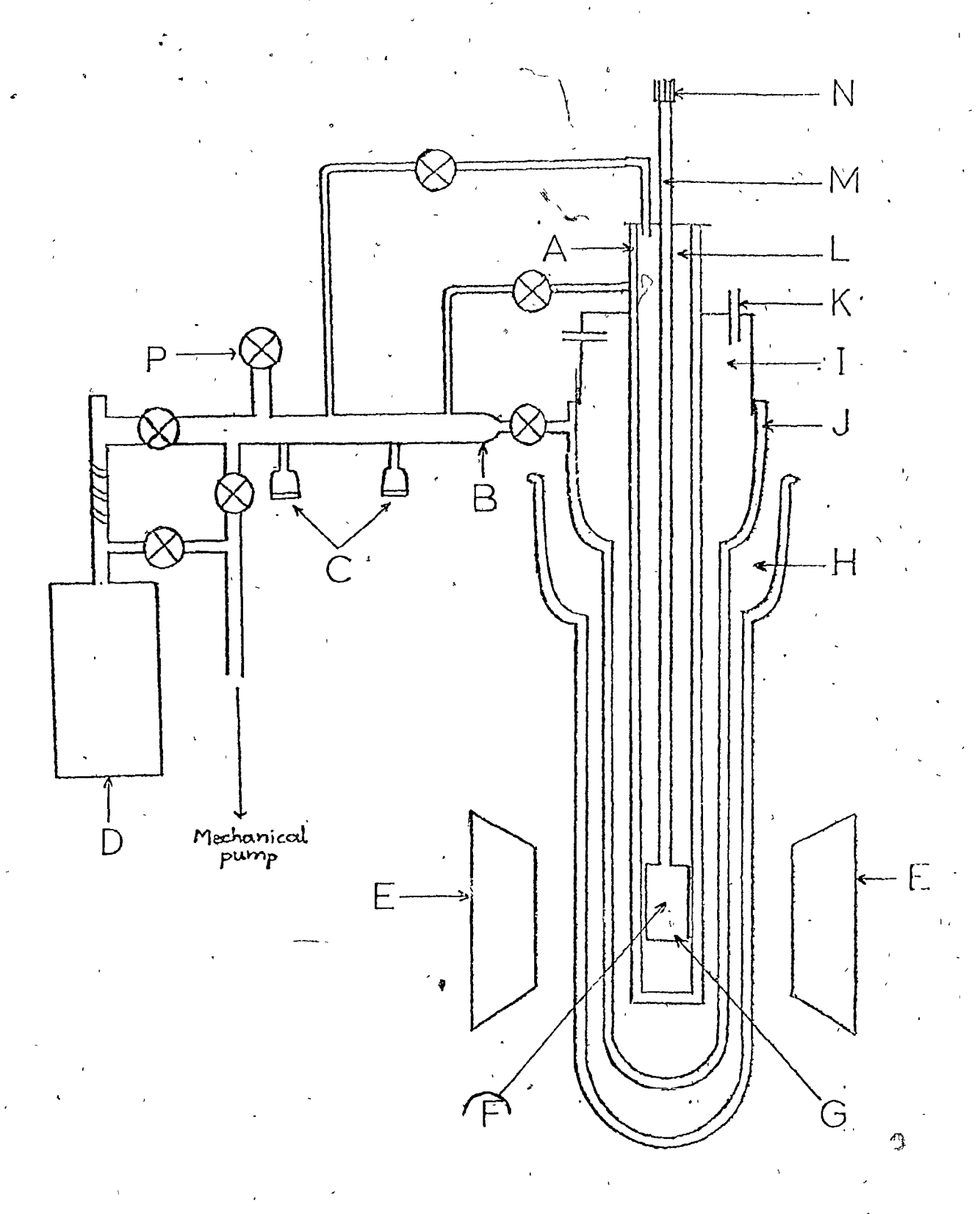


Fig. 4 The cryostat

The isolation space A, i.e. the inner wall space of the exchange gas chamber, allows one to thermally isolate the sample space from the outer space or to control the cooling rate monitoring the pressure. This exchange gas chamber is placed in a dewar I, which serves as a liquid helium reservoir when measurements are taken down to about 5 °K or it is just open to the air when these are taken in the temperature-interval 80 to 295 °K. The inner-wall space J of this dewar is connected to the diffusion pump D through the tube B. The outer dewar H, is filled with liquid nitrogen when measurements are taken. This one also consists of a double wall evacuated space.

As it has already been said, the temperature range in which the measurements were carried out was extended from 5 °K to 295 °K and it was divided, in accordance with the method used to establish the required temperature, into two parts, the 80 - 295 °K region and the 5 - 80 °K one. To obtain the former, the spaces A and L are filled with helium gas with pressure of some Torr; this pressure is kept low in order to have slow temperature variance. The space J is filled with nitrogen gas to the atmospheric pressure. Finally, the space H is filled with liquid nitrogen.

For the next temperature region (i.e. 5 - 80 °K), we repeat the above procedure and when the temperature of the sample falls to 80 °K, then the nitrogen gas is pumped out from the space J by the mechanical and diffusion pumps. When the pressure comes down to $\sim 5 \times 10^{-4}$ Torr, then liquid helium is transferred to the space I.

Temperature control of the above mentioned range is obtained by supplying with just sufficient electrical power the heater G to bring the sample region to the desired temperature. The temperature is determined by

a temperature sensor which is a GaAs diode, type TG-100P of Lake Shore Cryotronics, useful in all the interesting temperature range. This diode is located in the back side of the platform in which the sample is and in the same distance as the sample from the heater. The calibration of this diode is presented on fig. 5, where the temperature vs. voltage has been drawn.

3.4. The Magnet Control System

For the Hall effect measurements, a Harvey-Wells electromagnet with pole faces 30 cm in diameter and a pole gap of 7.5 cm was used. The maximum field intensity of this electromagnet is 10 kG. The power supply for it is of model HS-1365 from Harvey-Wells Corp. Its panel operating controls include the field set controls with visual indication of the field current and a field reversing switch.

The calibration of this magnetic field has been made by the students S. Kovalski and S. Berger using an NMR Probe. The calibration graph is shown in fig. 6 where the magnetic field in kG vs. current in amperes is given.

3.5. The Electrical Measuring Circuit

Two geometric forms have been used for measuring the resistivity and the Hall voltage of the present samples. The form of fig. 7.a has been used for the samples Al and A2. Efforts to improve the accuracy of the measurements led to the form of fig. 7.b which is widely used. The latter form has been adopted for the samples Bl and B2.

Fig. 8 shows a diagram of the electrical measuring circuit. A regulated current source supplies the current which is read by a milliammeter.

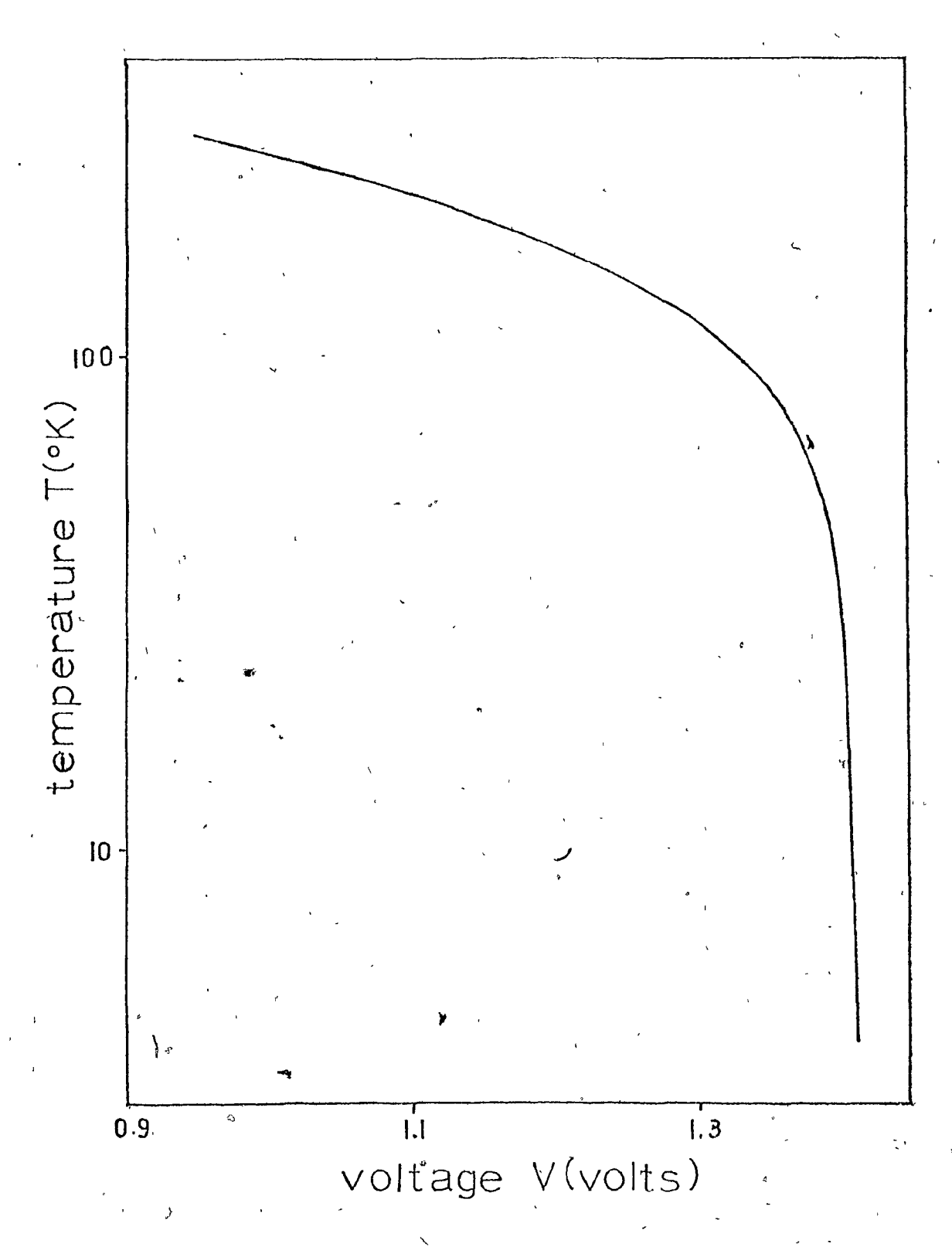


Fig. 5 Temperature sensor calibration

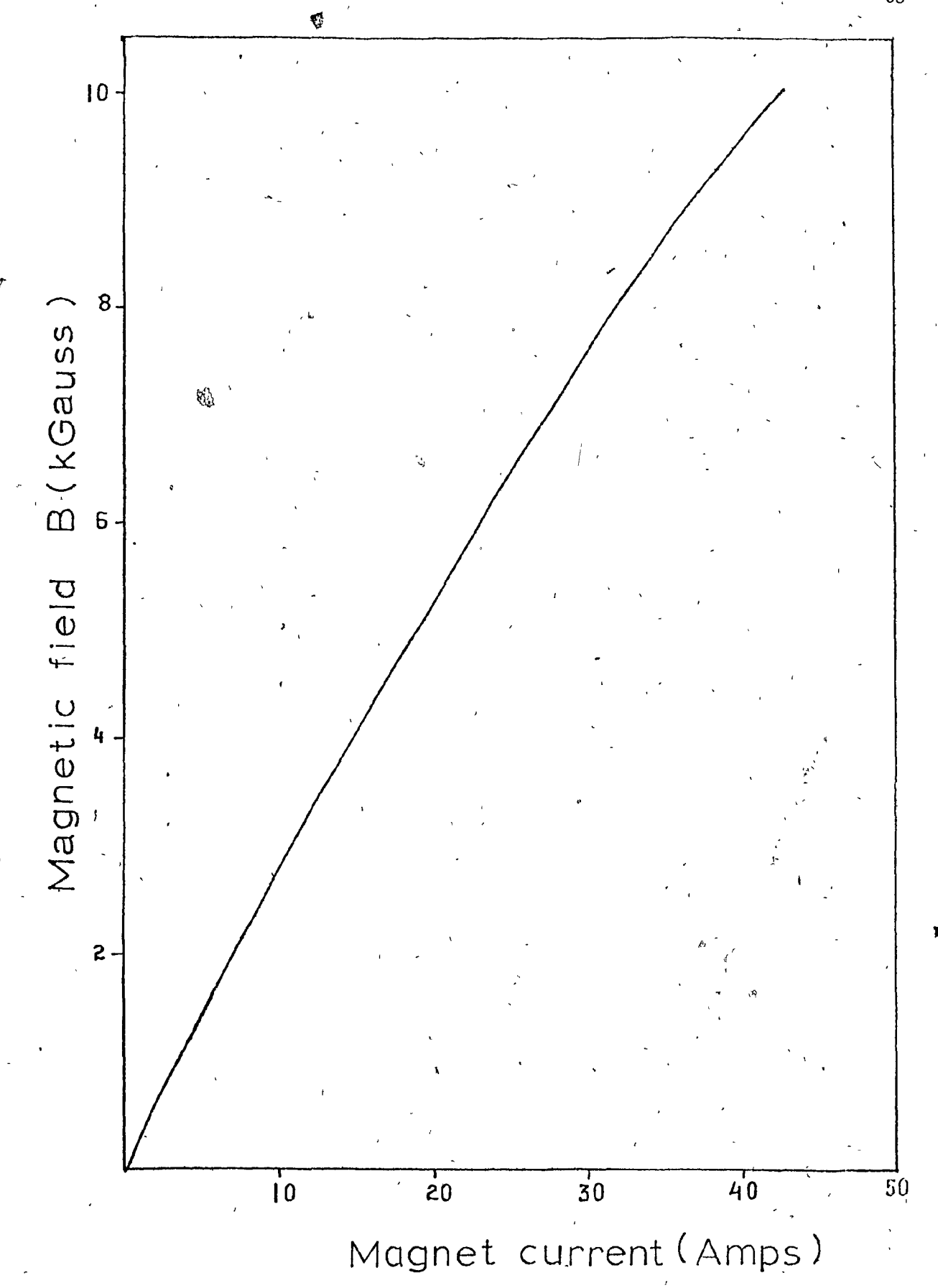


Fig. 6 Magnetic field calibration

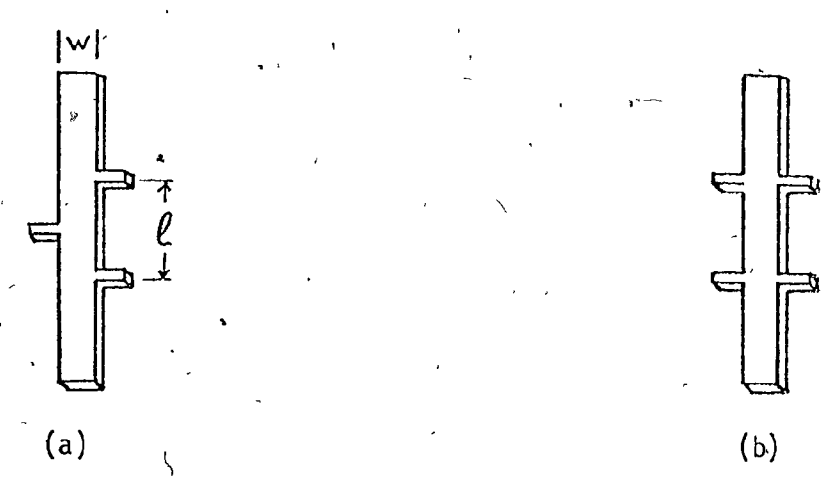


Fig. 7 Geometric forms of the samples

(a): for samples Al and A2

(b): for samples B1 and B2

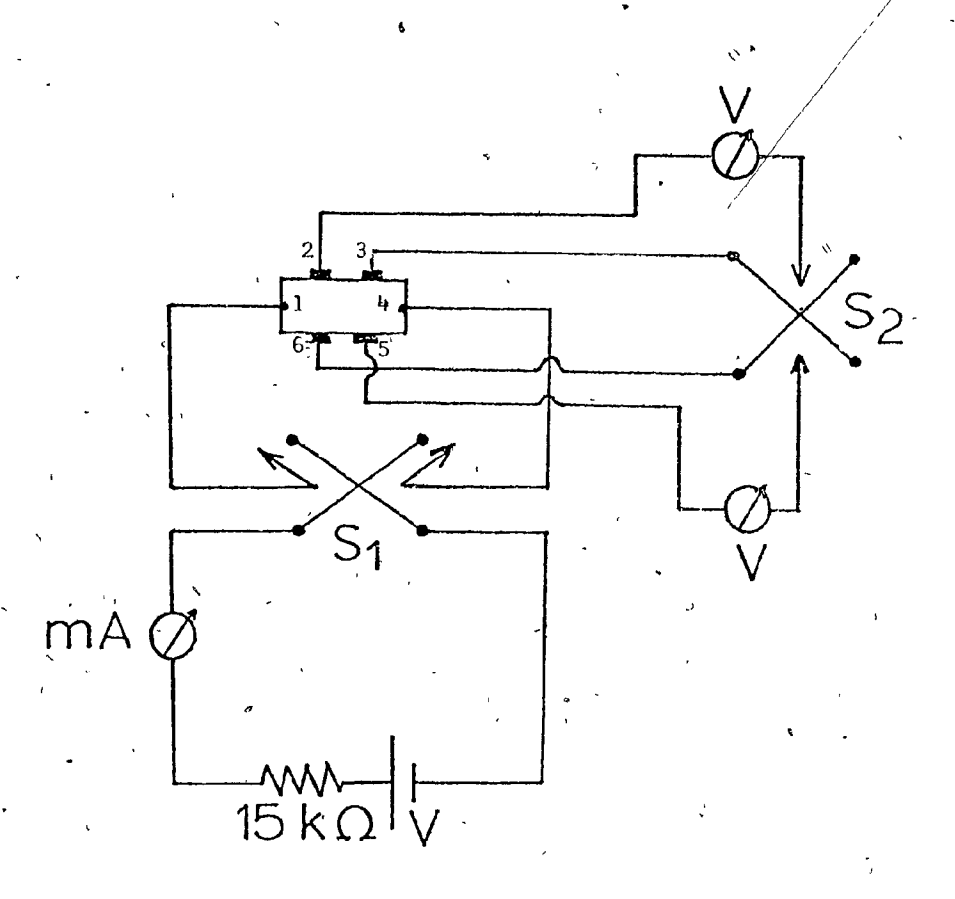


Fig. 8 Electrical measuring circuit

A resistor of 15 k Ω is connected in series with the sample in order to keep the current constant. The switch S_{1} permits current reversal. Two digital voltmeters measure both voltages, the one by which the resistivity is calculated, and the Hall voltage by appropriately connecting the switch S_{2} .

The heater is placed at the lowest side of the platform and it is supplied with current by a regulated current source. The temperature is determined from the calibrated tables of the GaAs diode temperature sensor (fig. 5). The latter is connected with a power supply and a voltmeter. The power supply has a multiple range of supplied current of 0.001, 0.010, 0.055, 0.137 and 1.35 mA. The calibration of fig. 5 has been made for a current of 0.010 mA.

3.6. Preparation of the Samples

In this paragraph, we discuss briefly the procedure followed to grow the studied materials. It should be noted here, that the whole part of the growth (set-up and procedure) was made by J. Auclair (Research Assistant).

All the four studied materials were nominally undeped GaAs single crystals, grown on semi-insulating Cr-doped GaAs substrates (homoepitaxial growth) under low pressure and changing only the growth temperature and the flow rate of the reactants. Mechanically polished semi-insulating Cr-doped GaAs, provided by Laser Diode Labs, Inc. were used as substrates. Prior to growth, they were etched in a 3:1:1 solution of $H_2SO_4:H_2O_2:H_2O$ for approximately 15 minutes. After being rinsed in distilled water and in methanol, they were placed on the graphite pedestal and inserted into the reactor.

The pressure, under which the growth was taking place was kept constant at 0.3 Torr during the whole growth process. The reactants used

for the studied crystals were trimethylgallium (TMG), 5% A_sH₃ in ultra pure H₂ and as a carrier gas Pd-purified H₂, in agreement with the first group of chemical reactions, mentioned in paragraph 2.5.

The conditions under which the growth of the studied semiconductors took place are presented in Table 1 for each sample. Under these conditions, the grown samples exhibited excellent surface morphology.

3.7. Hall Measurements

Each sample, as it was obtained, was cut by sandblasting to take the mentioned forms (fig. 7a,b). Prior to contact evaporation the sample was etched in a 3:1:1 solution of $H_2SO_A:H_2O_2:H_2O$ for 2O-3O sec. After being rinsed in distilled water, the sample was kept in methanol. Good ohmic contacts were made to n-type GaAs by evaporation of an alloy Au:Ge (12% by weight of Ge) adding Ni about 5-10% of the weight of the alloy Au-Ge. It has been found that the presence of the nickel helps the contacts to be uniform over the surface of the semiconductor. The evaporation was carried out in a low pressure of $\sim 10^{-6}$ Torr. After the evaporation, the contacts were annealed for 1 min at 500 °C in N_2 atmosphere.

Since the contacts have been made and annealed, the sample was ready for Hall measurements. This was mounted on a copper plate, electrically isolated from the sample, and wires were silverplated on the contacts. To make the resistivity and Hall measurements, the following process was exercised.

The voltage V_X and V_X across the contacts (2,3) and (5,6), respectively (the latter, where applicable, see fig. 8) was measured for zero magnetic field and for both directions of the current. Averaging them, the voltage V_X was obtained. Then the resistivity was calculated using

TABLE I

Sample	Growth Temperature (°C)	Ratio A _s H ₃ /TMG	TMG Flow (cc/min)	A _s H ₃ Flow (cc/min)
A1 (650	5:1	4. 8	15.0
. A2	635	5:1	5.2	17.4
В1	625	5:1 [,]	,5.2	17.4
, B2;	625	6.5:1	5.2	22.6
, a	,		, 1	-

eq. (2.29) and the conductivity by eq. (2.30).

The Hall voltage was determined by measuring the voltages V_1 across the contacts (2,6) and V_2 across the contacts (3,5). (For the shape of fig. (7.a) V_1 and V_2 were the voltages across the contacts (2,6) and (3,6), respectively). These measurements were taken with the magnetic field on, off and reverse. Also, for both directions of the current.

If we denote V_1^F , V_1^0 and V_1^R the above voltage V_1 for the magnetic field on, off and reverse, respectively, then the Hall voltage across these contacts for the given direction of current is given by,

$$V_{H} = \frac{(V_{1}^{F} - V_{1}^{0}) - (V_{1}^{R} - V_{1}^{0})}{2} = \frac{V_{1}^{F} - V_{1}^{R}}{2}$$
(3.1)

The minus sign between the two subtracts in the middle term of eq. (3.1) comes from the fact that if $V_1^F > V_1^O$, then $V_1^R < V_1^O$.

By eq. (3.1), we note that this Hall voltage is independent of the V_1^0 , which means that any assymetry of the contacts (especially the large assymetry of the shape of fig. (7.a)) does not affect the Hall voltage, if it is calculated by this method. By the same method, the Hall voltage across the other two contacts is measured and then the same is repeated for reverse current. Finally, the average Hall voltage V_H calculated by averaging these four "partial" ones.

From the Hall voltage V_H , the Hall coefficient R_H is calculated by the eq. (2.35), the mobility μ by eq. (2.36) and the ratio $\frac{1}{R_H e}$ which is equal to the carrier concentration n, if the Hall factor r_H is assumed to be unit. The dimensions of the samples are given in Table II. All the above steps were repeated for the whole temperature range.

TABLE II

Sample	Length & (cm)	Width w(cm)	Thickness t(μm)
Al,	0.420	0.520	7.0
A2	0.400	0.520	6.0
B1	0.445	0.472	2.2
B2	0.445	0.472	, 2.1
٢			

The maximum current used was up to 1 mA and the magnetic field was $4 \text{ kG } (=4.10^{-5} \text{ y} \cdot \text{sec} \cdot \text{cm}^{-2})$. The field dependence of the Hall coefficient was checked up to 7 kG and it was found to be independent. For low temperatures, the current was reduced in order to avoid the heating of the sample.

By this process, measurements of the electrical properties were made for a given sample supplied by Laser Diode Labs. Inc. and the error between the results and that given by the manufacturing company data was approximately 8%.

EXPERIMENTAL RESULTS AND DISCUSSION

As we have already said, Hall measurement were made for temperature ranging from 5 °K to 295 °K for four n-type GaAs samples grown by Organometalic-Vapor Phase Epitaxy (OM-VPE) under the conditions listed in Table I. In the previous chapter, we discussed the experimental process under which these measurements have been obtained.

The need to know the optimum growth conditions, such as temperature and arsine to metalorganics ratio for future work, has been the motivation to electricially characterize the grown materials.

The present work is limited to this electrical characterization, that is, to determine resistivity, Hall mobility, carrier concentration and their temperature dependence, as well as the total impurity content, and it does not enter to details about crystal growth. In this chapter, the results are listed and they are interpreted in terms of existing theories of electrical conduction in semiconductors.

4.1 Temperature Dependence of Resistivity, Hall Coefficient and Hall Mobility

The results of measurements of the temperature dependence of the resistivity, Hall coefficient and mobility are plotted in figures 9, 10, and 11, respectively.

From fig. 9, we see that the resistivity has a small minimum just under the room temperature, and as the temperature decreases, the resistivity increases with a finite slope, until at approximately 30 $^{\circ}$ K, where the slope changes and vanishes at \sim 20 $^{\circ}$ K. Therefore, the conductivity at

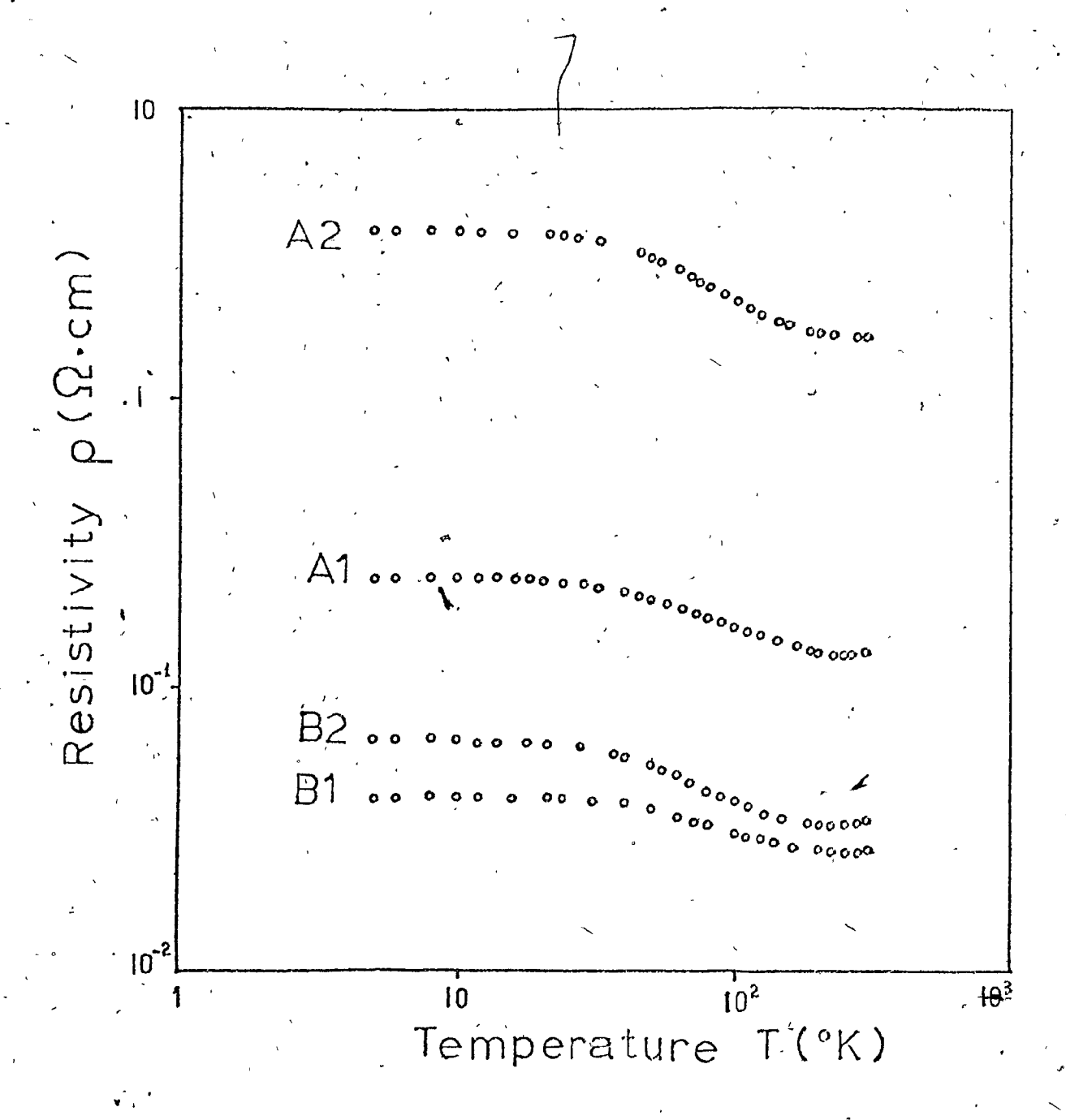


Fig. 9 Resistivity vs. temperature

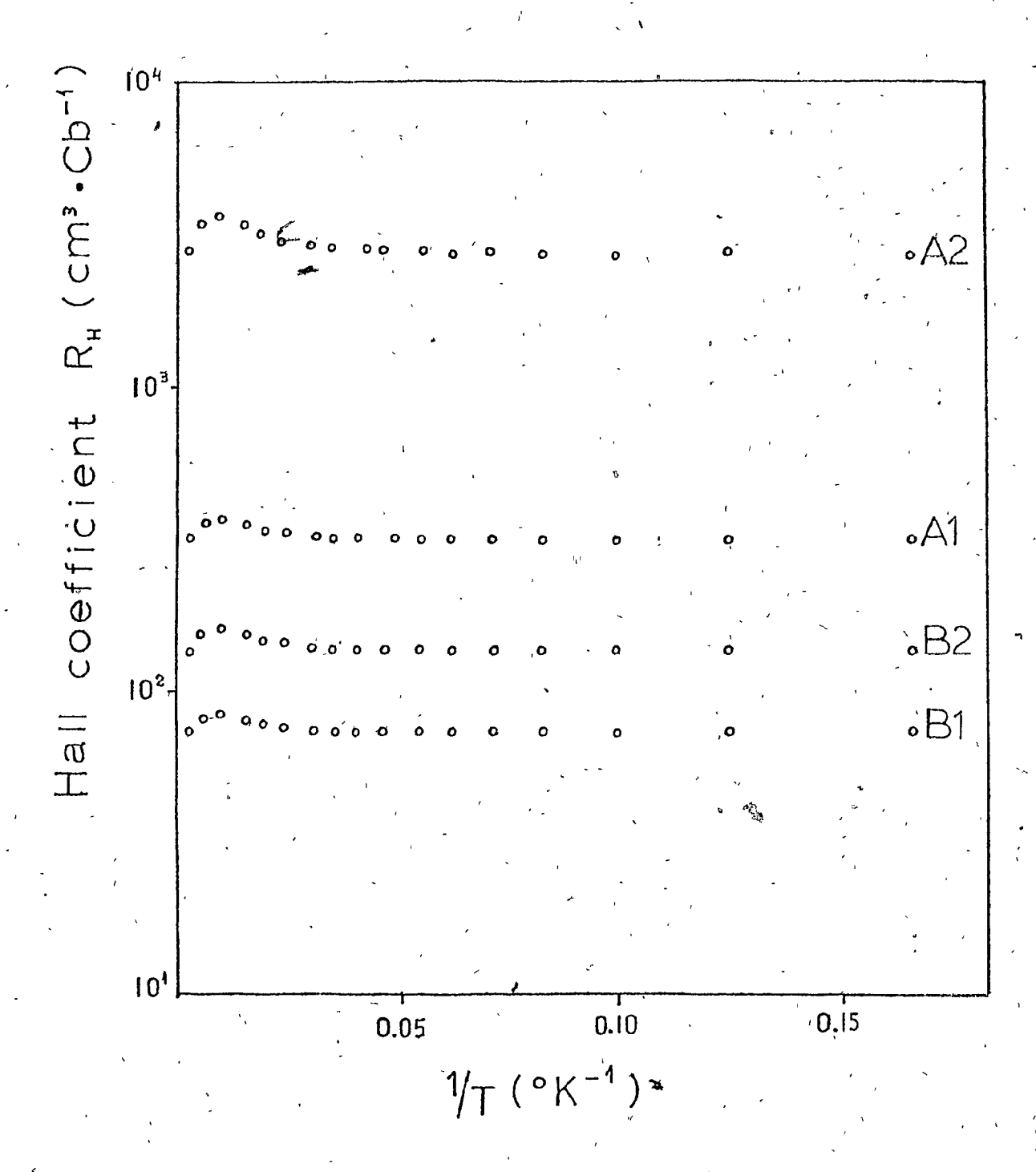


Fig. 10 Hall coefficient vs. inverse temperature

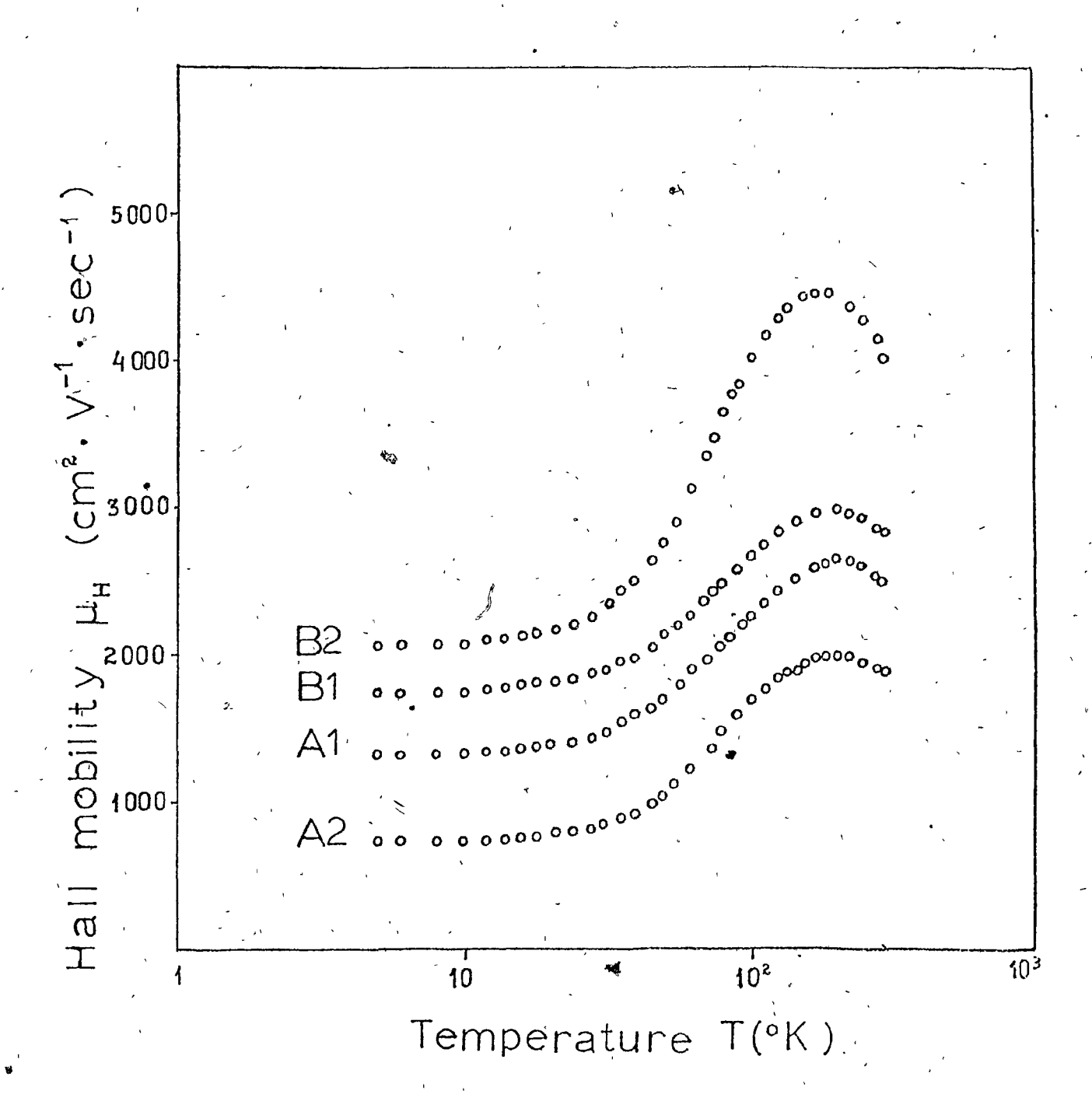


Fig. 11 Mobility vs. temperature

Wery low temperatures is constant.

In fig. 12, the resistivity vs. I/T is plotted. Here, we can see this behaviour more clearly. This change of the slope at very low temperatures is related to impurity conduction ⁽⁴⁾. Moreover, the constant conductivity shows that this conduction is metallic-like. Therefore, the two Hubbard bands D° and D^{-(7,9)} have merged, resulting in $\epsilon_2 = 0$ (see eq. (2.12)) and there is a finite conductivity even at very low temperatures.

As it has been said, the number of carriers n at the exhaustion range, as well as at the metallic behaviour, is constant and equal to N_D - N_A , where N_D , N_A are the donor and acceptor concentrations, respectively. The carrier concentration is given in terms of the Hall ceofficient R_H . We see from fig. 10 that the Hall coefficient is constant at very low temperatures. As the temperature increases, it has a small maximum at $\sim 90~^\circ K$ and then it falls again for higher temperatures at the same value it has for very low temperatures.

Many authors (4,9,11,21,22) attribute this behaviour to two-band conduction. According to them, the maximum occurs at the transition from one band to another. By two-band conduction, it is meant that the electrons move either in the conduction band or in the impurity band $D^{-(9)}$, which resulted from the overlap of the wave functions of the impurity atoms (see paragraph 2.2). The former case occurs at relatively high temperatures, while the latter at very low ones. In the intermediate temperature range both affect the conductivity and this is the temperature range where the Hall coefficient deviates from its constant value.

On the other hand, some other authors (21,23) consider the change of the Hall factor r_H to explain the maximum of the Hall coefficient. They

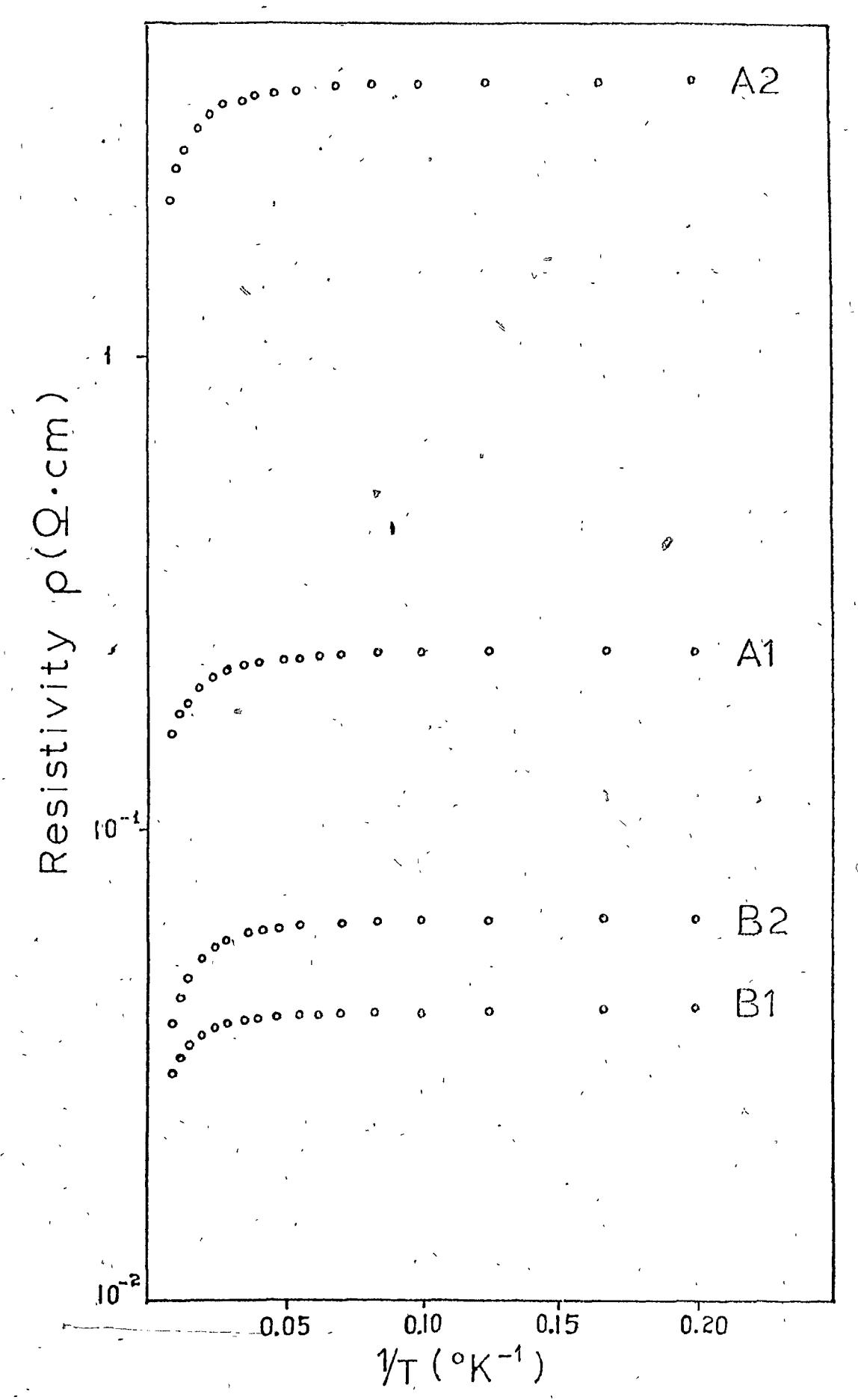


Fig. 12 Resistivity vs. inverse temperature

remain always in the conduction band, that is, the impurity band has merged completely with the conduction band.

To find the appropriate process for our case, let us see the temperature dependence of the other parameters. We have already discussed the resistivity behaviour. Concerning the mobility, we see from fig. 11 that starting from room temperature the mobility increases as the temperature decreases reaching a maximum at ~ 200 °K and as the temperature goes on decreasing, then the mobility decreases also and finally it becomes constant at very low temperatures, where it has a mobility whose value is between one third and one half of the maximum.

We believe that all these data combined result in a two-band conduction: at very low temperatures, all the electrons are in the impurity band where the mobility is constant. (The same for the conductivity, as long as all the electrons remain in the impurity band (eq. 2.16)). This mobility is lower than the mobility in the conduction band.* The difference in the mobility is because of the effective mass difference, the latter being dependent on the shape of the bands. Obviously, the conduction band does not have the same shape as the impurity band. As the temperature increases, some electrons "jump" from the impurity to the conduction band with a resultant higher mobility and hence higher conductivity. So, for a temperature range we have a mixture of two contributions to the mobility and conductivity. This is the range where the Hall coefficient deviates from its constant value. In this case, the Hall coefficient is given by (4,22)

^{*} For the hopping process, this mobility has been found to be much lower $^{(24)}$.

$$R_{H} = \frac{n_{i}\mu_{i}^{2} + n_{c}\mu_{c}^{2}}{e(n_{i}\mu_{i} + n_{c}\mu_{c})^{2}}$$
(4.1)

In eq. (4.1), the symbols have the known meanings with the subscripts i, c denoting the impurity band and conduction band, respectively. Also, in deriving eq. (4.1) $r_{\rm H}$ = 1 is assumed. The same value of $r_{\rm H}$ will be assumed in the rest of the present work, since the impurity band plays a dominant role even at moderate temperatures and as we have said, for distorted bands the Hall factor approaches the unit. In any case, the error resulting from this assumption will not be more than 5 - 10% which is within our experimental error.

For very low temperatures, when all the electrons are in the impurity band, eq. (4.1) becomes

$$R_{H} = \frac{1}{n_{i}e}$$
 (4.1a)

while for high temperatures

$$R_{H} = \frac{1}{n_{c}e} \tag{4.1b}$$

and all the electrons are in the conduction band.

From eq. (4.1a) or (4.1b), we can find the total electron concentration

$$n = N_{D} - N_A = \frac{1}{R_H \cdot e}$$

where $\mathbf{R}_{\dot{H}}$ is the constant value of the Hall coefficient.

As long as this transition occurs, the mobility in the conduction band remains constant. This comes from the fact that the energy given to the crystal by heating it is spent for the carrier excitation from the impurity to the conduction band and not for increasing the velocity of the electrons already existing in the conduction band as the Brooks-Herring (B-H) formula, eq. (2.23), or Falicov-Cueyas (F-C) formula, eq. (2.25) presuppose.

Taking the derivative of eq. (4.1) with respect to the temperature, we find that the maximum occurs when $n_i^{\mu} = n_c^{\mu}c$. Since $\mu_i^{\mu} < \mu_c$, then $n_i^{\mu} > n_c$, therefore, even at ~ 90 °K, the carrier concentration in the impurity band is significant, which means that the ionization energy ΔE_D (or ϵ_1 from eq. (2.12)) is not too small as one would expect regarding the metallic behaviour and high concentration of the carriers, at least for the three samples, A1, B1 and B2. In the next paragraph, an approximate evaluation of this activation energy is made.

4.2. Calculation of the Activation Energy ϵ_1

For the two-band conduction, the effective conductivity is the result of the two components σ_i and σ_c where σ_i , σ_c are the conductivities in the impurity and conduction bands, respectively. Then, the conductivity is given by

$$\sigma = \sigma_1 + \sigma_C \tag{4.2}$$

If for the two terms of the right hand part of eq. (4.2), the eq. (2.16) is applied, then eq. (4.2) becomes

$$\sigma = n_{i} |e| \mu_{i} + n_{c} |e| \mu_{c}$$
 (4.3)

The term n_c represents the fraction of the total electron concentration which is in the conduction band. This can be approximated for low temperatures, as

$$n_{c} = (N_{D} - N_{A}) \cdot \exp(-\varepsilon_{1}/kT) \qquad (4.4)$$

Substituting eq. (4.4) into eq. (4.3) and having that $n_i = n - n_c$, we take

$$\sigma = n[1 - \exp(-\frac{\varepsilon_1}{kT})]|e|\mu_1 + n \exp(-\frac{\varepsilon_1}{kT})|e|\mu_C$$
 (4.5)

In eq. (4.5) we notice that the term $n|e|\mu_i$ is the conductivity for very low temperatures σ_i^0 , where all the electrons are in the impurity band. This conductivity, as we can see from fig. 9, is constant for a limited temperature range. Also, the term $n|e|\mu_c$ is the conductivity σ_c^0 when all the electrons are in the conduction band. This, of course, happens for higher temperatures. Yet, the latter case is not as simple as the former, because the mobility μ_c is constant, as we have already said, only for a limited temperature range when there still are electrons in the impurity band, while for higher temperatures ionized impurity and polar optical scattering mechanisms affect this mobility. Hence, we must find an optimum temperature, where these scattering mechanisms have not started yet and at the same time all (or nearly all) the carriers are in the conduction band.

From the figures 9, 10 and 11, we find that the temperature of 150 °K meets the above requirements. First, the Hall coefficient at this point is near the constant value, which means that almost all the electrons are in the conduction band and second, at this temperature, the mobility changes slope, which means that the normal scattering mechanisms start to operate. Thus, taking as $\sigma_{\bf i}^{\bf 0}$ the conductivity at 5 °K and as $\sigma_{\bf c}^{\bf 0}$ the conductivity at 150 °K, eq. (4.5) becomes

$$\sigma' = \sigma_1^0 [1 - \exp(-\varepsilon_1/kT)] + \sigma_C^0 \exp(-\varepsilon_1/kT)$$
 (4.6)

We note that eq. (4.6) resembles eq. (2.12). Eq. (4.6) can be written as

$$\frac{\sigma - \sigma_{i}^{0}}{\sigma_{c}^{0} - \sigma_{i}^{0}} = \exp(-\varepsilon_{1}/kT)$$
(4.7)

If the term
$$\int_{\sigma_{c}^{0} - \sigma_{i}^{0}}^{\sigma - \sigma_{i}^{0}} is \text{ plotted vs. 1/T in semi-log graph, then the slope}$$

If the term 0 - 0 is plotted vs. 1/T in semi-log graph, then the slope will give the activation energy. This is done in fig. 13 (a,b,c,d) for the samples Al, A2, Bl, B2, respectively. We notice that as the temperature increases, this slope increases too, although the error in calculating ϵ_1 for high temperatures is more significant than that of low temperatures, since eq. (4.4) holds for low T. In any case, an estimation of ϵ_1 can be made. Its values for low and high T are given in Table III for each sample. Therefore, we conclude that the impurity band has a width of ϵ_1 and that the impurity band does not overlap the conduction band, but its highest edge is about 2 meV from the conduction band. Photoluminescence studies near the band-edge (ϵ_1) at 2 °K are consistent with this result; the

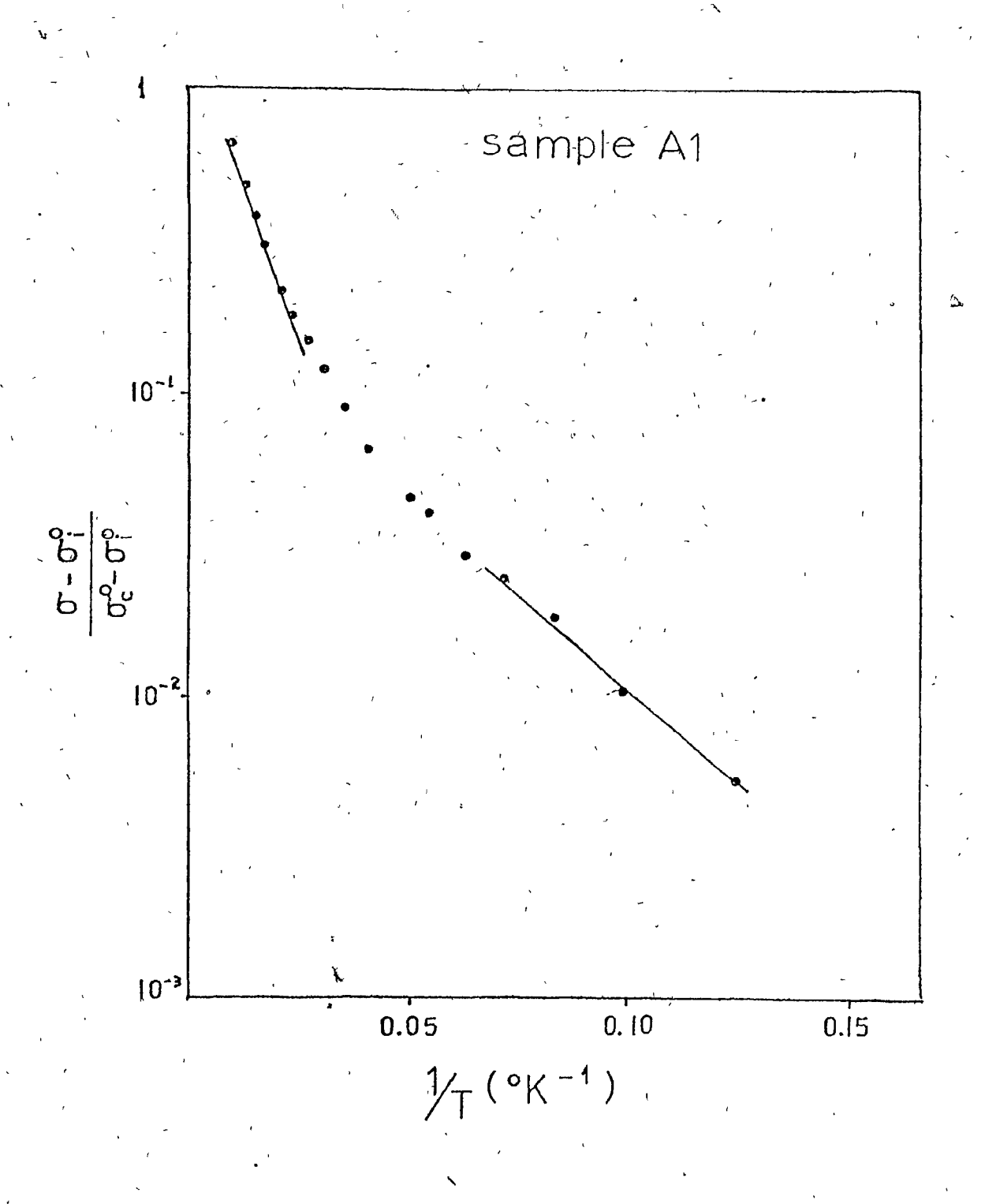


Fig. 13.a $\frac{\sigma - \sigma_i^0}{\sigma_c^0 - \sigma_i^0}$ vs. inverse temperature

for sample Al

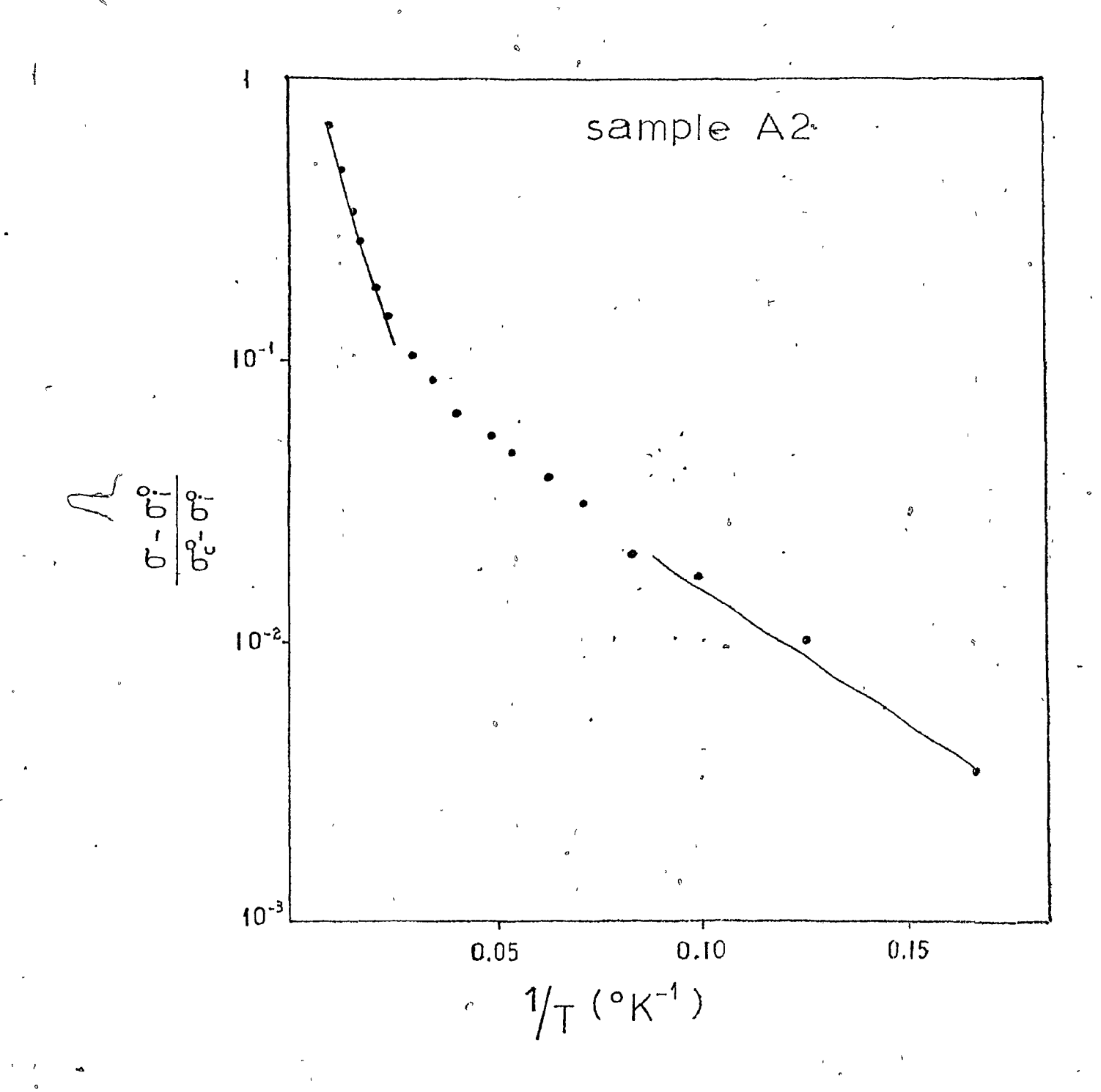


Fig. 13.b
$$\frac{\sigma_i^0 - \sigma_i^0}{\sigma_c^0 - \sigma_i^0}$$
 vs. inverse temperature

for sample A2

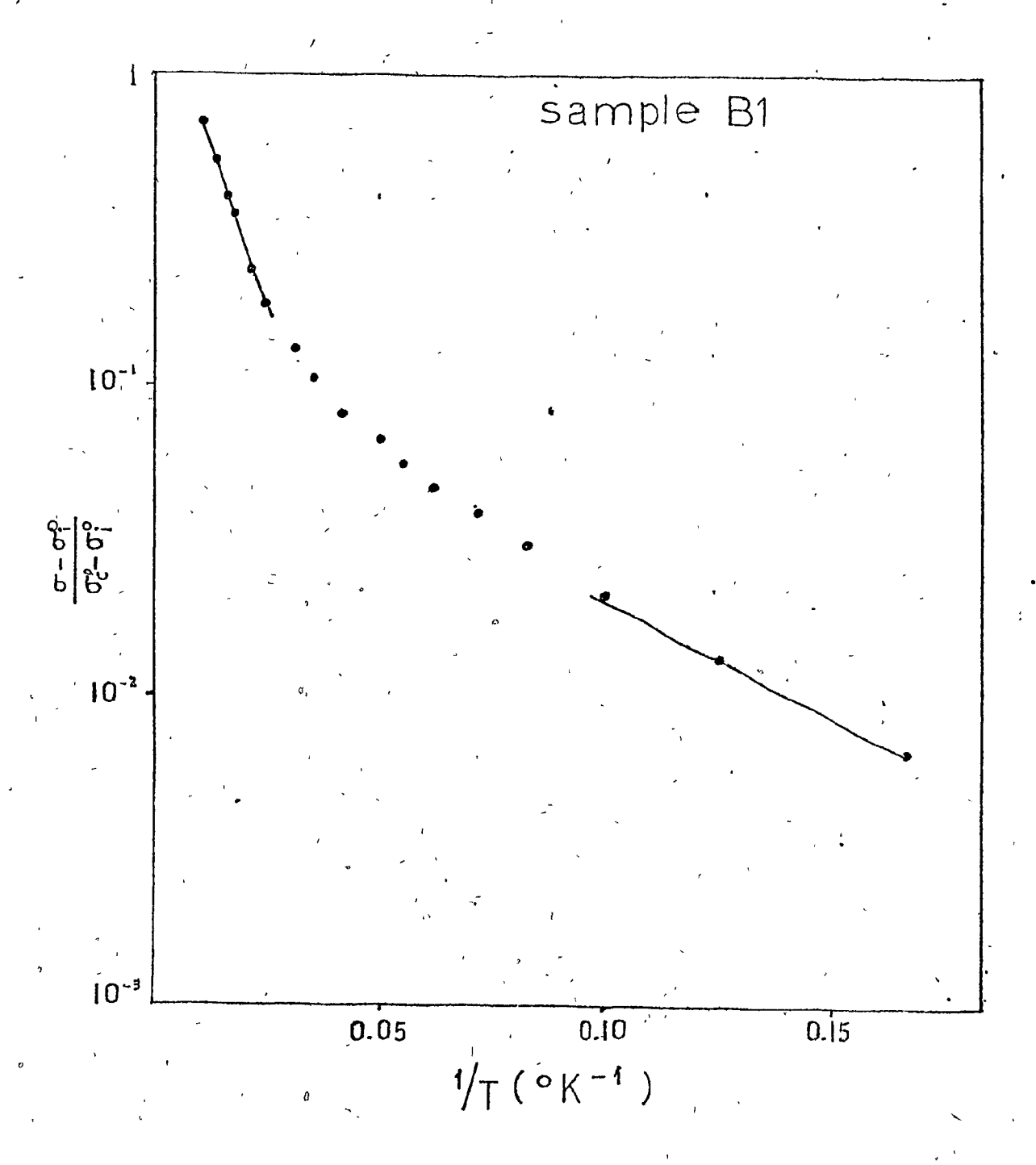
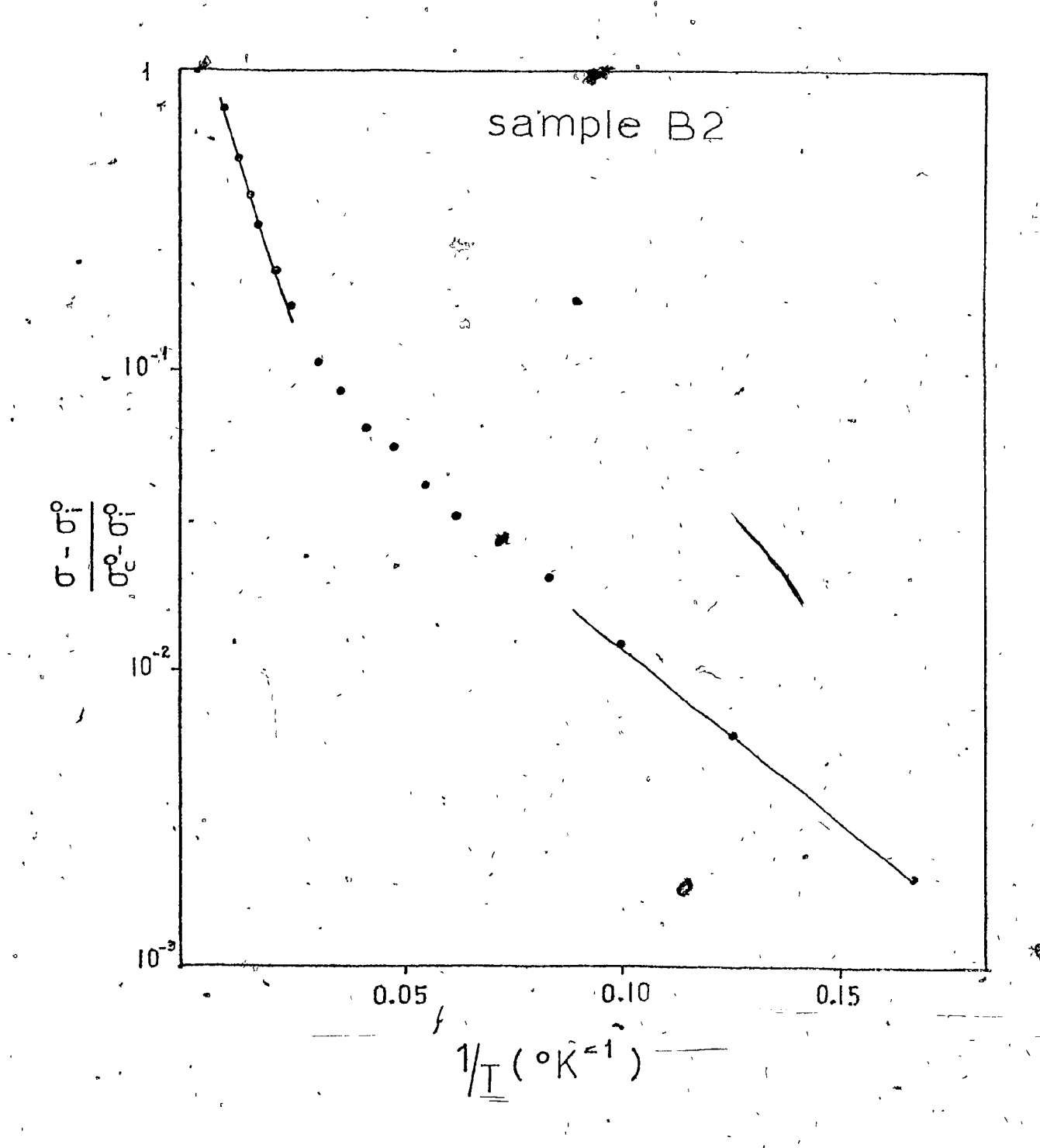


Fig. 13.c. $\frac{\sigma - \sigma_i}{\sigma_c^0 - \sigma_i^0}$ vs. inverse temperature

for sample Bl



4

Fig. 13.d
$$\frac{\sigma - \sigma_i^0}{\sigma_c^0 - \sigma_i^0}$$
 vs. inverse temperature

for sample B2

photoluminscence shows a broad line whose half-width is approximately 7 meV and whose peak is at 6 meV below the conduction band for sample A2.

TABLE III

Sample	$\sigma_{i}^{0}(\Omega^{-1}\cdot cm^{-1})$	$\sigma_{\mathbf{c}}^{0}(\Omega^{-1}\cdot\mathbf{cm}^{-1})$	Activation Er Low T	nergy ε _l (me V) High T
ĄΊ	4.25	7.25	° 2.75	7.50
A2	0.262	, 0. 56	1.95	9.30
ВЛ	24.2	35.7	1.50	8.00
B2	15.46	29.0	2.40	9.35

4.3. Calculation of Total Impurity Concentration and Compensation

Usually the total impurity concentration and compensation is calculated by the (B - H) formula, eq. (2.23) or by the (F - C) formula, eq. (2.25), applying them at $\sim 80~\text{c}^{(23,25)}$. In our case, this is not applied since more than half of the electrons are still in the impurity band. We said in the preceding paragraph that at $\sim 150~\text{c}$ K the mobility due to scattering mechanisms changes slope and we see that it actually becomes constant for a small temperature range, beyond which it decreases. The decrease is attributed to the polar optical scattering, hence, we may assume that at room temperature only this mechanism operates. Moreover, at 200 °K, all the electrons have already been activated to the conduction band, and thus the

ionized impurity scattering has some effect on the mobility.

Assuming that at 200 °K both scattering mechanisms contribute to the mobility, the mobility due to ionized impurity scattering $\mu_{\rm I}$ can be found, applying Matthiessen's rule, eq. (2.28), if that due to polar optical scattering is known. The mobility $\mu_{\rm PO}$ at 200 °K can be found by comparing it to the measured mobility at room temperature. We know that (see eq. (2.19))

$$\mu_{P0}^{\alpha}(e^{\frac{\Theta}{T}} - 1) \text{ for } T < \Theta$$

0 is the Debye temperature and is equal to 417 °K for GaAs. Therefore,

$$\frac{\mu_{PO}^{200}}{\mu_{PO}^{295}} = \frac{e^{417/200} - 1}{e^{417/295} - 1} = 2.265$$
 (4.8)

By Matthiessen,s rule

$$\frac{1}{\mu_{\text{eff}}} = \frac{1}{\mu_{\text{PO}}} + \frac{1}{\mu_{\text{I}}}$$

then

$$\mu_{I} = \frac{\mu_{P0} - \mu_{eff}}{\mu_{P0} - \mu_{eff}}$$
 (4.9)

If in eq. (4.9) we put the value of μ_{p0} for 200 °K as it is obtained by eq. (4.8) and as μ_{eff} the measured at 200 °K, then the μ_I for this temperature can be found.

Although at high temperatures the difference-between the (F-C) and the

(B-H) formulas is insignificant $^{(15)}$, we shall use the former, since this is more appropriate for strongly compensated semiconductors. If $m^* = 0.07m_0$ and $\chi = 13$, then the eq. (2.25) becomes

$$\mu_{\rm I} = A \frac{2.11 \cdot 10^{18}}{2N_{\rm A}} \, {\rm T}^{3/2} \tag{4.10}$$

where

$$A = \frac{1}{\ln(1 + \eta) + \eta(1 + \eta)^{-1}}$$

and η is given by eq. (2.26).

Using the value of $\mu_{\rm I}$ for 200 °K, the acceptor concentration can be found by eq. (4.10) and the total impurity concentration by N $_{\rm I}$ = 2N $_{A}$ + n. The compensation is given by K = $\frac{N_{A}}{N_{D}}$.

Table IV contains all the parameters used to these calculations, as well as their results.

Having finished with the analysis of the measurements, we can now make some observations. All the GaAs layers grown under the conditions listed on Table I have a large number of impurities of both types and they exhibit metallic-like behaviour at very low temperatures. This is expected for the samples Al, Bl and B2, since their free carrier concentration exceeds the critical value given by Mott's criterion, eq. (2.11), and which is $\sim 1.6 \cdot 10^{16}$ for GaAs. Yet, for the sample A2, this behaviour is explained if the total donor concentration is taken into consideration, as Fritzsche (8) proposes.

TABLE IV .

SAMPLE	CARRIER CONCENTRATION n (cm ⁻³)	_μ(¢m²/\ 200-°K	/·sec) 295 °K	DONOR CONCENTRATION ND (cm-3)	ACCEPTOR CONCENT NA (cm-3)	COMPENSATION K
А٦	2.10 ¹⁶	2630	2500	. 1.4.10 ¹⁷	1.2.10 ¹⁷	0.86
A2	2.2.10 ¹⁵	2020	1910	1.21.10 ¹⁷	1.19.10 ¹⁷	.0.98
B1	8.65-10 ¹⁶	2980	2860	2.18·10 ¹⁷	1.31.10 ¹⁷	0.60
B2	4.65.10 ¹⁶	4435	4020	1.23.10 ¹⁷	7.6·10 ¹⁶	0.62

Moreover, we found that this metallic behaviour only occurs at very low temperatures since the impurity band has not merged with the conduction band. On the contrary, we found that there is an activation energy ε_1 which separates these two bands and whose value is between 1.5 and 2.8 meV for very low temperatures and that the impurity band has a width between 5 and 7 meV. The lowest ε_1 is for the sample with the largest donor concentration, which is reasonable, since, as the donor concentration increases, the activation energy tends to vanish. Yet, the next lower ε_1 is for the sample A2, whose donor concentration is comparable with the other samples. Probably this is due to high acceptor concentration of this sample. This contradicts with the observation of Davis and Compton for Ge(11), who found that ε_1 decreases as the donor concentration increases. In any case, this needs further investigation especially for extreme low temperatures.

Concerning the crystal-growth technique, it is noted that high quality materials were obtained with good value of mobility, especially the samples Al, Bl and B2. It is seen from Table IV that the lower the compensation and total impurity concentration are, the higher the mobility. The high impurity concentration at the present limits the application of such crystals for high electronic technologies, although they can be used for high-efficiency solar cells.

CONCLUSION

The experimental set-up for electrical characterization of semiconductors was described. The main part of this characterization is the Hall-effect measurement. By the latter, the electrical characterization of n-type GaAs single crystals was made. These crystals were grown by Organometallic-Vapor Phase Epitaxy (OM-VPÉ) on semi-insulating Cr-doped GaAs substrates. It was found to our surprise that these crystals exhibit metallic behaviour at very low temperatures which indicates that the donor concentration exceeds the critical value given by Mott, even for the sample with the relatively low free carrier concentration. This temperature dependence of the resistivity, Hall coefficient and mobility was explained with the two-band conduction, and from the temperature dependence of the conductivity, the activation energy ε_1 was found and the impurity band width was estimated.

The total impurity concentration, as well as the compensation ratio, were estimated by the Falicov-Cuevas formula concerning the mobility due to ionized impurity scattering. This was calculated at 200 °K, assuming that two scattering mechanisms operate at this temperature, the one due to ionized impurity scattering and the other due to polar optical scattering.

The above analysis of the electrical properties of the samples investigated shows that with the present employed crystal-growth technique, the obtained crystals have a high impurity concentration but their mobility is good for this number of impurities. Although these crystals can be used for high-efficiency solar cells, they will find limited application for other devices due to their high impurity concentration. Further investi-

gation is needed in order to grow single crystals with lower number of impurities and therefore higher mobility.

The present work was directed to the electrical characterization of the grown samples. The error in the electrical measurements is estimated to be 5 - 10% but this does not alter our conclusions. Since the crystals grown under the present conditions have a high impurity concentration and a high compensation, these samples can be used as models for liquid, amorphous and other disordered semiconductors, and may give opportunities to extend the theoretical knowledge about these materials, especially when measurements are taken at extreme low temperatures.

REFERÊNCES

- 1. Int. Symp. GaAs and Related Compounds. Inst. Phys., London.
- 2. Sze, S.M. Physics of Semiconductor Devices (John Wiley and Sons, New York 1969) p. 30.
- 3. Nag, B.P. Electron Transport in Compound Semiconductors. (Springer-Verlag, Berlin 1980) p. 90, 91.
- 4. Mott, N.F. and Twose, W.D. Adv. Phys. 10, 107(1961).
- 5. Mott, N.F. Philos. Mag. 6, 287(1961).
- 6. Mott, N.F. and Zinamon, Z. Rep. Prog. Phys. 33, 881(1970).
- 7. Hubbard, J. Proc. Roy. Soc. (London) A277, 237(1964).
- 8. Fritzsche, H. Philos. Mag. 42, 835(1980).
- 9. Fritzsche, H. J. Phys. Chem. Solids 6, 69(1958).
- 10. Mott, N.F. Adv. Phys. <u>16</u>, 49(1967).
- 11. Davis, E.A. and Compton, W.D. Phys. Rev. 140, A2183(1965).
- 12. Blatt, F.J. Physics of Electronic Conduction in Solids (McGraw-Hill, New York, 1968).
- 13. Petritz, R.L. and Scanlon, W.W. Phys. Rev. 97, 1620(1955).
- 14. Brooks, H. Adv. Electron. Elect. Physics, 7, 85(1955).
- 15. Falicov, L.M. and Cuevas M., Phys. Rev. <u>164</u>, 1025(1967).
- 16. Blatt, F.J. Solid State Phys. 4, 199(1957).
- Manasevit, H.M. Appl. Phys. Lett. <u>12</u>, 156(1968).
 Manasevit, H.M. and Simpson, W.I. J. Electrochem. Soc. <u>116</u>, 1725(1969).
- 18. Rai-Choudhoury, P.M. J. Electrochem. Soc. <u>116</u>, 1745(1969).
- 19. Ito, S., Shinohara, T. and Seki, Y. J. Electrochem. Soc. <u>120</u>, 1419. (1973).

- 20. Braslau, N., Gunn, J.B. and Staples, J.L. Solid State Electron., 10, 381(1967).
- 21. Emel'yanenko, O.V., Lagunova, T.S., Maronchuk, I.E. and Chugueva, Z.I. Sov. Phys.-Semicond. 11, 1376(1977).
- 22. "Basinski, J. and Olivier, R. Can. J. Phys. <u>45</u>, 119(1967<u>)</u>.
- 23. Vul, B.M., Zavaritskaya, E.I., Voronova, I.D. and Rozhdestvenskaya, N.V.

 Sov. Phys.-Semicond. 5, 829(1971).
- 24. Miyao, M. and Narita, S. J. Phys. Soc. Japan 42, 128(1977).
- 25. Wolfe, C.M., Stillman G.E. and Dimmock, J.O. J. App. Phys. <u>41</u>, 504 (1970).